

HEPSY-95-05
November 1995

DECAYS OF b QUARK

TOMASZ SKWARNICKI

Department of Physics, Syracuse University

Syracuse, NY 13244, USA

E-mail: tomasz@uhep2.phy.syr.edu

ABSTRACT

Importance of studies of b quark decays and experimental status of various measurements are discussed.

*To appear in the Proceedings of
the 17th International Conference on Lepton-Photon Interactions
Beijing, China, August 1995*

1. Introduction

1.1. Physics Goals

The existence of three generations of quark weak doublets has been well established experimentally. The origins, however, of different quark (and lepton) generations, of their mixing in charged weak currents, and of their mass spectrum have not been understood. Furthermore, some elements of the mixing matrix (the Cabibbo-Kobayashi-Maskawa matrix) involving quarks of the third generation (b and t) are poorly measured. Decays of the b quark play a strategic role in the determination of the CKM parameters. The latter is very important for understanding the nature of CP violation discovered in decays of s quark, and for tests of the CKM matrix unitarity (is there a fourth generation ?). After the recent discovery of the top quark, the b quark is no longer the heaviest known quark, but it is still the heaviest among those creating hadrons. As such, it plays a very important role in studies of strong interactions. Its heavy mass and relatively long lifetime, make decays of the b quark also an interesting place to search for rare decays due to non-standard interactions. In this paper we will concentrate on recent experimental results concerning rare decays and determination of the CKM parameters. The latter necessarily overlaps with understanding strong interaction phenomena interfering with weak decays.

1.2. Experimental Environments

At present b quark decays are under investigation with large statistics at three different colliders: CESR producing $B\bar{B}$ pairs in decays of the $\Upsilon(4S)$ resonance just above the $e^+e^- \rightarrow B\bar{B}$ threshold, LEP producing $b\bar{b}$ pairs in Z^0 decays, and Tevatron producing $b\bar{b}$ pairs in $p\bar{p}$ collisions. Various production aspects at these machines are compared in Table 1. The CLEO-II experiment at CESR enjoys the highest achieved

Table 1. Various parameters characterizing experimental environments at three colliders active in producing b quarks. Explanation of the symbols: σ —cross section, \mathcal{L} —luminosity, β —velocity of b quarks, $\beta\gamma c\tau$ —mean decay path, f —fractions of b hadron species produced.

Quantity	$\Upsilon(4S)$ (CESR)	Z^0 (LEP)	Tevatron
$\sigma(b\bar{b})$ nb $^{-1}$	1.1	9.2	~ 30000 $ y < 1$ (~ 6000 $p_t > 6$ GeV)
$\sigma(b\bar{b})/\sigma(q\bar{q})$ %	~ 30	~ 20	~ 0.1
\mathcal{L}^{peak} cm $^{-2}$ s $^{-1}$ 10 $^{-31}$	33.0	1.1	2.5
$\int \mathcal{L} dt$ pb $^{-1}$ analyzed in pipeline	2400 1000	~ 75 > 13	~ 65 > 20
$b\bar{b}$ pairs 10 6 analyzed	2.6	0.7	~ 2000 (~ 200) †
β	~ 0.07	~ 1	~ 1
$\beta\gamma c\tau$ μm fragmentation background	30	2600	500
spatial separation of b and \bar{b}	no $E_B = E_{beam}$	some $\overline{E_B} \sim 0.7 E_{beam}$	large
$f_{B^+} \approx f_{B^0}$	0.5	yes	~ 0.4
$f_{B_s^0}$	—	~ 0.1	~ 0.1
f_{Λ_b}	—	~ 0.1	~ 0.1
main advantage	simple production, statistics	vertexing, one b at a time	cross-section, vertexing

† These numbers correspond to the central region, $|y| < 1$, with high transverse momentum of b quark, $p_t > 6$ GeV (the number in parentheses).

collider luminosity and a simple production mechanism. Both, charged tracks and photons, are detected with good efficiency and resolution. Since no fragmentation particles are produced, energy of reconstructed B 's can be constrained to the beam energy which provides for a powerful reconstruction technique. On the other hand since two B mesons are produced almost at rest, detection of a detached secondary B decay vertex is not possible on event by event basis. Also, decay products from the two B 's in the event populate the entire solid angle. At LEP momentum given to b hadrons is appreciable, thus the decay products from the two b hadrons produced are easily separated into back-to-back hemispheres. A large decay path gives rise to many important analysis techniques. Even though the $b\bar{b}$ cross section is much larger than at the $\Upsilon(4S)$ resonance, a high energy of the beam limits achievable luminosity. In

view of the forthcoming end of the Z^0 running at LEP, statistics should be considered the main limiting factor for the LEP experiments. The huge production cross-section is the main asset of the Tevatron experiments. A large background cross-section is the main obstacle to overcome in b experiments with hadronic beams. Specialized triggering is needed to limit data acquisition to manageable rates. So far, the results from Tevatron have been mostly limited to channels containing high p_t muons. Again, vertexing is an important selection tool.

1.3. General structure of b quark decays in the Standard Model.

Since decays of the b quark to the t quark and W^- are kinematically forbidden in the first order, the b quark decays to the c or u quark and virtual W^- that turns to a pair of leptons or quarks (Fig. 1a). The decays to the c quark are strongly favored by the values of the CKM elements ($|V_{cb}|^2/|V_{ub}|^2 \sim 10^2$). Decays to down-type quarks, s or d , are forbidden by the GIM mechanism (Fig. 1b). In the second order, b can decay to virtual t and W^- that immediately recombine to the s or d quark (so called loop or penguin decays). The decays to the s quark are favored by the CKM elements ($|V_{ts}|^2/|V_{td}|^2 \sim 10^1$). To conserve energy, something must be emitted from these interactions: a photon, a gluon that turns to quarks, or a neutral Z^0 that turns to a pair of quarks, leptons or neutrinos (Fig. 1c). The latter decays can also occur via a box diagram with two charged W 's exchanged between the heavy and the lighter fermion lines (Fig. 1d).

All of the above are spectator decays, since the other quark in the initial hadron does not participate in the short distance disintegration of the b quark. Analogous decays exist for non-spectator decays of B_q mesons in which the b quark and its lighter partner q annihilate to virtual bosons (Fig. 1e-i). Annihilation processes are suppressed by the smallness of the B decay constant. Furthermore, since the b quark is heavy, helicity suppression is very effective in annihilation to leptons. In the first order, only B_u^- can annihilate (Fig. 1e). However, this process is strongly disfavored by the smallness of the CKM element involved (V_{ub}). Annihilation of B_d^0 and B_s can occur in the second order by the inverted penguin or box diagrams (Fig. 1g-i). The annihilation of B_s is preferred by the CKM element ($|V_{ts}|^2/|V_{td}|^2 \sim 10^1$). As a combined effect of the suppression factors mentioned above, the annihilation processes in B meson decays are expected to be very rare. Therefore, the spectator decays of the b quark are easier to detect. The first order spectator decays serve a measurement of the third column of the CKM matrix ($|V_{cb}|$ and $|V_{ub}|$), whereas the loop decays can be used to probe the third raw of the matrix ($|V_{ts}|$ and $|V_{td}|$).

An alternative way to determine $|V_{td}|$ and $|V_{ts}|$ from b interactions is to study $B^0\bar{B}^0$ and $B_s\bar{B}_s$ oscillations, produced by the box diagrams. Complex phases of the CKM elements can be accessed via CP violating phenomena expected in b quark decays. The above topics are the subject of separate papers presented at this conference. ¹

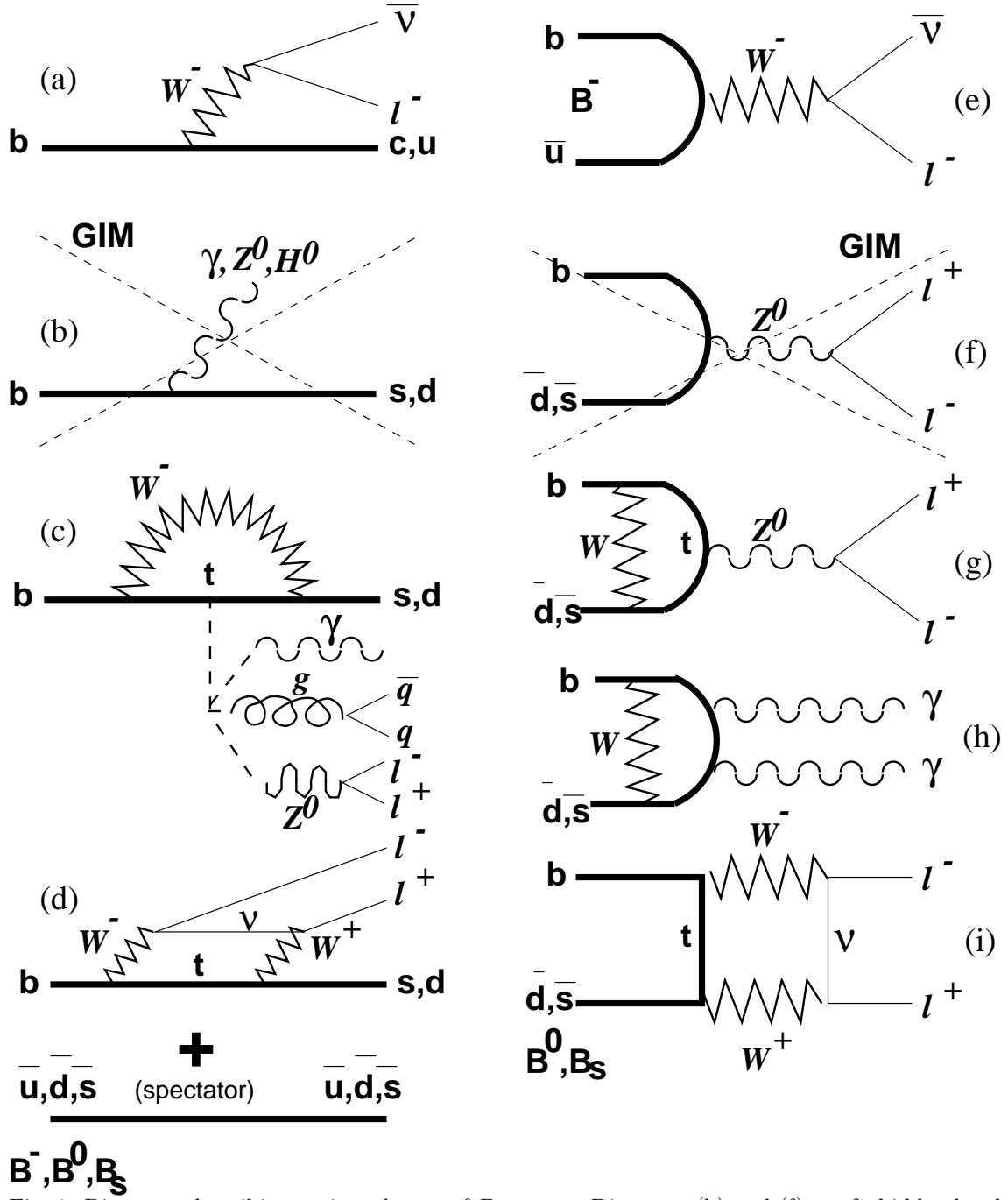


Fig. 1. Diagrams describing various decays of B mesons. Diagrams (b) and (f) are forbidden by the GIM mechanism. Any lepton line can be also replaced by quark line.

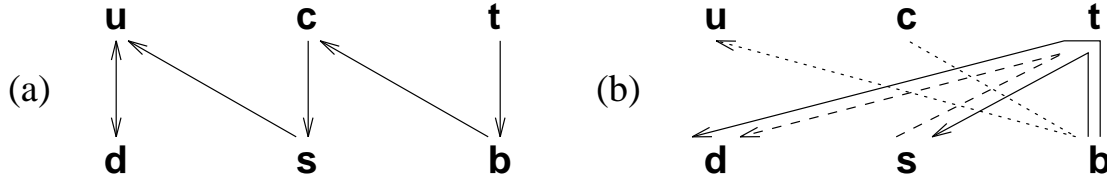


Fig. 2. Standard Model decays of quarks. (a) Dominant first order decays. (b) Second order quark transitions.

1.4. Decays of the b quark versus decays of the other quarks

Decays of down-type quarks are generally more interesting than decays of up-type quarks. Because of the quark mass pattern, up-type quarks can decay to a down type partner within the same generation (Fig. 2a). Thus, dominant decays of these quarks probe diagonal CKM elements that are known to be close to unity. These decays make the up-type quarks relatively short lived. In contrast, dominant decays of heavy down-type quarks change the quark generation. Because of the smallness of the off-diagonal CKM elements, the down-type quarks are relatively long lived. Decays of up-type quarks to the quarks of the other generations are rare and difficult to observe on top of the background from the dominant decays. Decays of the t quark to the s or d quark will be particularly difficult to observe. At present, the decays of the b and s quarks are the best experimental path to measure $|V_{ts}|$ and $|V_{td}|$.

The down-type quarks are also favored over the up-type quarks in the Standard Model loop decays (Fig. 2b). Since rate increases with the mass of the particle in the loop, exchanges of the t and b quarks dominate. Top as the heaviest quark has nothing to exchange in a virtual loop. The charm quark may decay to the u quark by exchanging the b quark, but rate for this decay is predicted to be extremely small since the c quark is short lived and the CKM factor ($|V_{cb} \cdot V_{ub}^*|^2$) is tiny. This leaves the b quark decays the only way to measure $|V_{cb}|$ and $|V_{ub}|$.

The strange quark can decay to the d quark by exchanging the t quark. As a down-type quark the s quark is longer lived. Also the CKM suppression is expected to be somewhat smaller ($|V_{td}| > |V_{ub}|$). Thus, the loop decays of the s quark are an interesting way to probe $V_{ts} \cdot V_{td}^*$.

Even a better access to these elements is provided by the loop decays of the b quark. There are two possible loop decays: to the s quark and to the d quark, thus each element can be probed separately. Since there is no CKM suppression in the intermediate $b \rightarrow t$ transition, the loop decays of the b quark are favored by very large factors compared to the s decays: $(b \rightarrow s)/(s \rightarrow d) \sim |(V_{tb} \cdot V_{ts}^*)/(V_{ts} \cdot V_{td}^*)|^2 \sim 1/|V_{td}|^2 \sim 10^4$, $(b \rightarrow d)/(s \rightarrow d) \sim 1/|V_{ts}|^2 \sim 10^3$. Also, the larger suppression of the dominant decays favors the b quark ($|V_{us}|^2/|V_{cb}|^2 \sim 30$). The large CKM suppression

factors can be overcome in s decay experiments by a higher quark production rate and a more controllable environment than in b decay measurements. However, the large CKM suppression is to be blamed for long distance strong interactions overwhelming almost all rare kaon decay channels.^a For example, the $K_L^0 \rightarrow \gamma\pi\pi$ decay, that can proceed via an electromagnetic penguin decay $s \rightarrow d\gamma$, is completely dominated by an internal W exchange producing a virtual π^0 or η that decays to $\gamma\pi\pi$.² In contrast, long distance strong interactions contribute only about 4% to channels produced by generic $b \rightarrow s\gamma$ decays.³ The short distance interactions are also expected to dominate $b \rightarrow d$ channels, though long distance contributions may be larger here.

Similarly, the loop decays of the b quark offer better sensitivity than the s quark decays for various contributions beyond the Standard Model, especially if mass dependent couplings are involved.

In conclusion, decays of the b quark are the most interesting among all decays of quarks.

2. Rare decays of b quark

2.1. Electromagnetic penguin decays

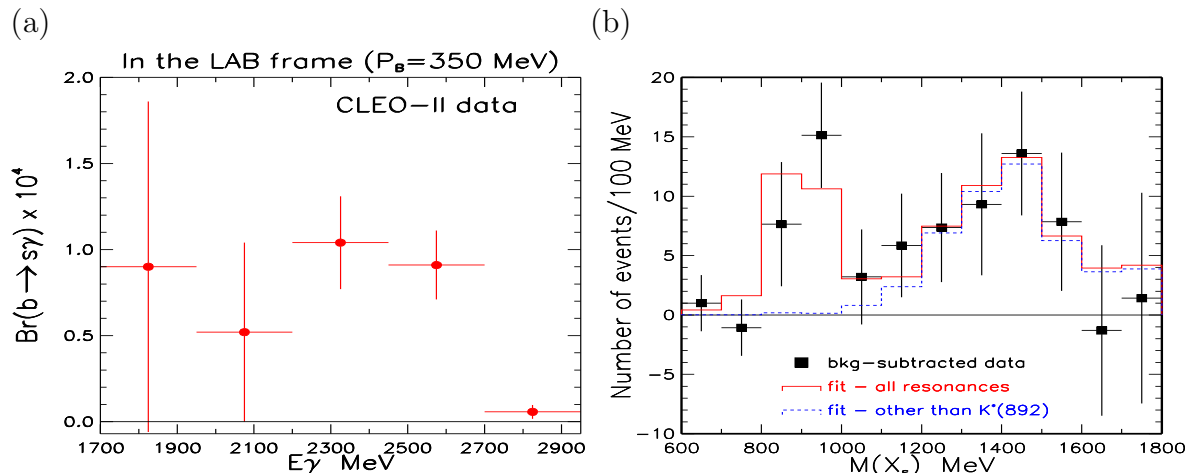


Fig. 3. Inclusive $b \rightarrow s\gamma$ signal in the CLEO-II data. (a) Measured photon spectrum averaged over the two analyses presented by CLEO.⁶ (b) Mass of hadronic system recoiling the photon.

2.1.1. $b \rightarrow s\gamma$

Electromagnetic penguin decays $b \rightarrow s\gamma$ were first observed by the CLEO-II experiment in the exclusive decay mode $B \rightarrow K^*\gamma$ in a sample of $1.5 \times 10^6 B\bar{B}$ pairs.⁴

^a The only exceptions are: $K^+ \rightarrow \pi^+\nu\bar{\nu}$ ($BR \sim 10^{-10}$), $K_L^0 \rightarrow \pi^0\nu\bar{\nu}$ ($BR \sim 10^{-11}$), and any CP violating pieces of rare or usual kaon decays.

Since then, CLEO-II has almost doubled the sample and presents an updated branching fraction for $B^0 \rightarrow K^{*0}\gamma$.⁵ Combining this result with the original measurement of $B^- \rightarrow K^{*-}\gamma$, we obtain: $Br(B \rightarrow K^*\gamma) = (4.5 \pm 1.0 \pm 0.6) \times 10^{-5}$.

CLEO-II recently published an inclusive measurement of the total $b \rightarrow s\gamma$ rate.⁶ Using the data sample of $2.2 \times 10^6 B\bar{B}$ pairs CLEO-II measured: $Br(b \rightarrow s\gamma) = (2.32 \pm 0.57 \pm 0.35) \times 10^{-4}$. With a quarter of that statistics, DELPHI sets an upper limit on this branching ratio, $< 6.3 \times 10^{-4}$ (90% C.L.), which is consistent with the CLEO-II value.⁷ The inclusive photon spectrum averaged over the two selection methods used by CLEO is displayed in Fig. 3a. As expected for quasi two-body decay, the spectrum peaks at $m_b/2$. Exact predictions for the photon energy distribution in this process are a subject of recent theoretical papers.^{8,9}

As illustrated in Fig. 3b, the CLEO-II inclusive measurement clearly indicates that the $b \rightarrow s\gamma$ process produces final states with masses also above the K^* resonance, though with the present experimental statistics it is not possible to disentangle various resonances in the higher mass region. The ratio of branching ratios, $R_{K^*} = Br(B \rightarrow K^*\gamma)/Br(b \rightarrow s\gamma) = (19 \pm 6 \pm 4) \%$, depends on the long distance strong interactions that follow the short distance penguin decay and create the K^* resonance. Additional complication arises from a possibility that the photon in this decay mode could also be generated by long distance strong interactions rather than the penguin decay (e.g. via formation of virtual J/ψ or ρ turning to the photon). The R_{K^*} ratio has been predicted by a number of phenomenological models and by QCD on lattice. Recent predictions are in rough agreement with the data.¹⁰

More interesting is the inclusively measured branching fraction since it does not depend on the hadronization process, and therefore reflects short distance interactions.^b A value of $|V_{ts}|$ can be extracted from a ratio of the measured branching ratio and the Standard Model prediction: $|V_{ts}|^2/|V_{cb}|^2 = Br(b \rightarrow s\gamma)_{meas.}/Br(b \rightarrow s\gamma)_{SM}$.^c Using the calculations by Buras et al.¹¹ we obtain:

$$\frac{|V_{ts}|}{|V_{cb}|} = 0.91 \pm 0.12(\text{experimental}) \pm 0.13(\text{theoretical})$$

in agreement with ~ 1.0 predicted by assuming unitarity of the CKM matrix. Larger estimates of the theoretical uncertainties can be found.⁸ The main theoretical error is due to the renormalization scale dependence since no complete next-to-leading order calculation exists. The theoretical error is already larger than the experimental one, thus complete next-to-leading order calculations would be very welcome.

Assuming the CKM matrix unitarity, the above ratio can be turned into an upper limit on the interactions beyond the Standard Model. Since the Standard Model diagram exchanges the two heaviest objects we know so far, the top quark and the W boson, the $b \rightarrow s\gamma$ process is very sensitive to a possible exchange of the non-standard particles, if such exist on a mass scale not too much larger than the scale

^b See Sec.3.1 for more detailed discussion of advantages of inclusively measured rates.

^c $Br(b \rightarrow s\gamma)_{SM}$ denotes here the Standard Model calculation that assumes $|V_{ts}|^2/|V_{cb}|^2 = 1$.

of the electroweak interactions. A large number of extensions of the Standard Model have been discussed in this context.¹² A typical example is a Two-Higgs-Doublet-Model in which the W in the penguin loop can be replaced by a charged Higgs. Since the Higgs contribution always increases the predicted rate, a lower limit on the Higgs mass can be obtained: $M_{H^-} > [244 + 63/(\tan \beta)^{1.3}]$ GeV, where $\tan \beta$ is a ratio of the vacuum expectations for the two Higgs doublets.^d For theoretically preferred large values of $\tan \beta$ the limit is almost constant. In supersymmetric models chargino and stop can be exchanged as well, that may add constructively or destructively to the total rate. Thus limits imposed on the supersymmetric parameters are somewhat complex. Naively, the charged Higgs, chargino and stop are either all heavy or all light.

2.1.2. $b \rightarrow d\gamma$

The main experimental difficulty in the search for $b \rightarrow d\gamma$ transitions is to distinguish them from more frequent $b \rightarrow s\gamma$ decays. CLEO-II searched for exclusive $B \rightarrow (\rho/\omega)\gamma$ decays.¹³ Because of the simplicity of the final state, the $B \rightarrow K^*\gamma$ background could be efficiently suppressed by kinematical cuts. With the present statistics no signal was found and an upper limit on $Br(B \rightarrow (\rho/\omega)\gamma)/Br(B \rightarrow K^*\gamma)$ was set. Neglecting possible long distance interactions, the latter ratio is equal to $\xi|V_{td}|^2/|V_{ts}|^2$, where ξ is a model dependent factor due to the phase space and $SU(3)_f$ breaking.¹⁴ Depending on the value of ξ :

$$\frac{|V_{td}|}{|V_{ts}|} < 0.64 - 0.76$$

It has been pointed out by many authors that long distance contributions may be significant for these decays.¹⁵ Separate measurements of B^- and B^0 decays, and of $\rho\gamma$ and $\omega\gamma$ will be helpful in isolating short and long distance contributions.

2.2. Rare exclusive hadronic decays

Gluonic penguin decays should give rise to various rare hadronic decay modes of the b quark. The total inclusive rate for such decays is expected to be much larger than for the electromagnetic penguin decays. Nevertheless these decays are more difficult to observe experimentally, since there is no common inclusive signature for these decays and exclusive branching ratios are small due to a large number of possible decay modes. Furthermore, many of these decay modes can be produced also by the $b \rightarrow uW^-$ decays which adds complexity to the analysis.

^dThis limit is valid for type-II Two-Higgs-Doublet-Models. See e.g. Ref 12 for more detailed discussion.

The main interest in rare hadronic decay modes is their future application in the determination of phases of the CKM matrix elements via measurements of the CP asymmetries.¹⁶ Interference of penguin and $b \rightarrow u$ amplitudes should give rise to direct CP violation in decays of charged and neutral B mesons. Interference of unmixed and mixed decays of B^0 to a CP eigenstate, like e.g. $B^0 \rightarrow \pi^+\pi^-$, is expected to produce indirect CP violation.

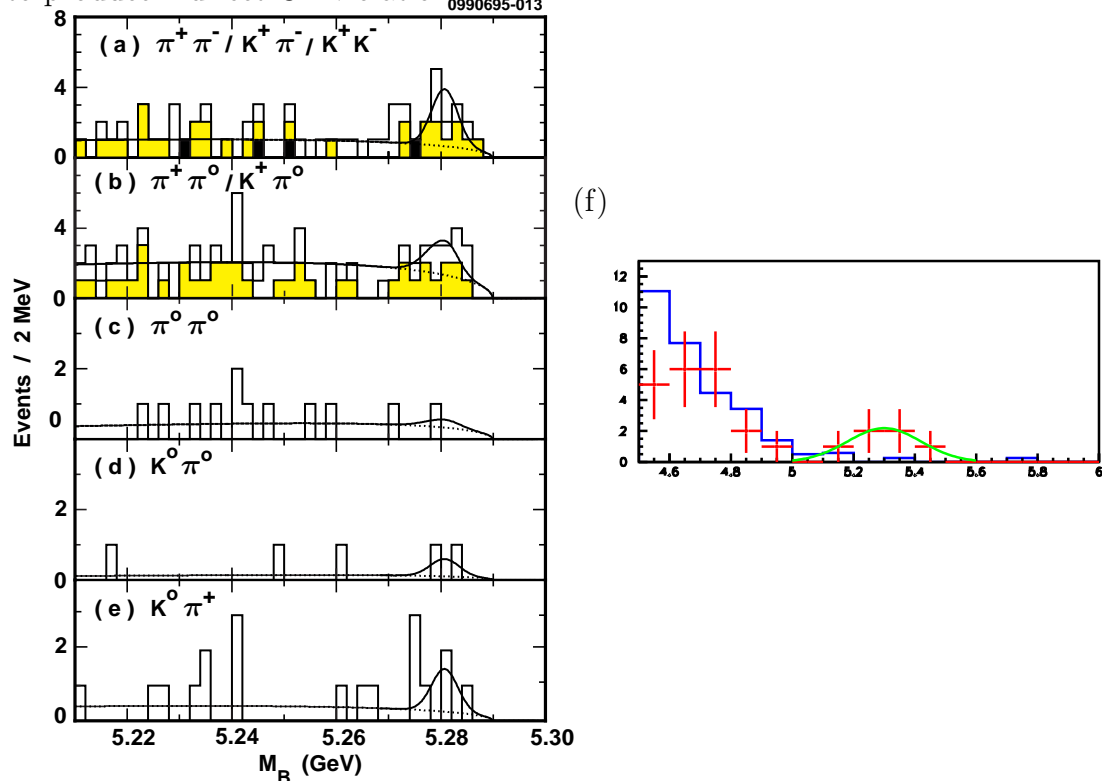


Fig. 4. Invariant mass of candidates for B decay products in searches for charmless hadronic decays. (a-e) A sample of CLEO-II results. Subsamples with preferred $K\pi/\pi\pi/KK$ interpretation are indicated by grey/unshaded/black histograms respectively. (f) Search for two-body and quasi two-body decay modes from DELPHI. Candidates for $\pi^+\pi^-/K^+\pi^-/K^+K^-/\rho^0\pi^-/K^{*0}\pi^-/K^-\rho^0/K^-\phi/K^+a_1^-$ are plotted together. The points with error bars represent the data and the histogram represents the estimated background from the $b \rightarrow c$ decays. Note that the DELPHI plot covers a 15 times larger range in M_B than the CLEO-II pictures. Neutral decay modes can be produced only by B^0 decays in the CLEO-II data, whereas at LEP they can come from either B^0 or B_s decays.

Three years ago CLEO-II reported¹⁷ the first evidence for a significant signal in B^0 decays to $h^+\pi^-$, where h^+ denotes either π^+ or K^- . An updated measurement¹⁸ with doubled the data sample (2.6×10^6 $B\bar{B}$ pairs) is $Br(B^0 \rightarrow h^+\pi^-) = (1.8^{+0.6+0.3}_{-0.5-0.4}) \times 10^{-5}$. About 17 signal events are observed. The most recent estimate of the $\pi^+\pi^-$ component of these decays is $Br(B^0 \rightarrow \pi^+\pi^-)/Br(B^0 \rightarrow h^+\pi^-) = (54 \pm 20 \pm 5)\%$. Since neither the $\pi^+\pi^-$ nor the $K^+\pi^-$ channel reaches three standard deviations in signal significance, CLEO-II quotes upper limits for these modes taken separately. There is an accumulation of events at the B mass for some other two-body and

quasi two-body decay modes as shown in Fig. 4a-e, though none of these peaks is statistically significant, thus upper limits are presented.

The LEP experiments have also searched for rare hadronic decay modes of B mesons. For example, DELPHI⁷ in a sample of $0.7 \times 10^6 b\bar{b}$ pairs produced observes a signal of 6 events over the estimated background of 0.3 events when all two-body and quasi two-body decays are put together. Half of these candidates are due to $h^+\pi^-$ events which is consistent with the rate measured by CLEO-II. As illustrated in Fig. 4f the B mass peak is much broader at LEP since B energy cannot be constrained to the beam energy as in the CLEO-II experiment. On the other hand backgrounds at LEP are smaller thanks to vertex cuts and separation of decay products from the two B mesons produced.

Upper limits reported by CLEO-II¹⁸, ALEPH¹⁹, DELPHI⁷, L3²⁰, and OPAL²¹ for various decay modes are illustrated in Fig. 5. Ranges of branching ratios predicted by theoretical models are also indicated. Thanks to the highest b quark statistics, the limits obtained by CLEO-II are the most stringent. L3 extended the searches to channels with η , and ALEPH and DELPHI to channels with multiplicities of up to 6 particles.

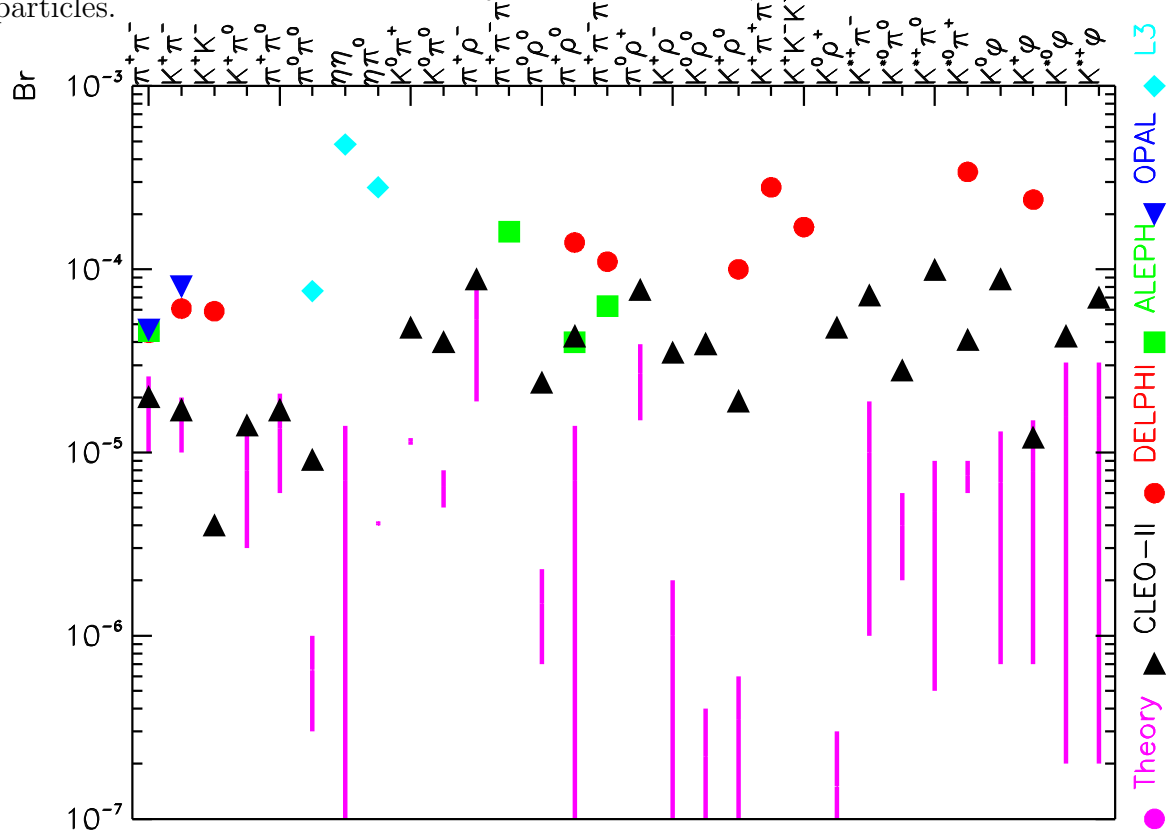


Fig. 5. Upper limits (at 90% C.L.) on branching fractions for charmless hadronic decays of B mesons obtained by various experiments. Vertical lines show a range of theoretical predictions when available. The predictions are model dependent. The CLEO-II analysis (triangles) is based on $2.6 \times 10^6 B\bar{B}$ pairs. The ALEPH (squares), DELPHI (circles) and L3 (diamonds) data samples included $0.7 \times 10^6 b\bar{b}$ events. The OPAL results (inverted triangles) are based on $0.4 \times 10^6 b\bar{b}$ pairs produced.

2.3. Search for inclusive $b \rightarrow s\phi$

Gluonic penguin decays which produce three strange quarks, $b \rightarrow sg$, $g \rightarrow s\bar{s}$ have no competition from the other decay mechanisms. Assuming that ϕ meson can be directly produced from these short distance interactions, as advocated by Deshpande and He,²² we can talk about $b \rightarrow s\phi$ decays. Such decays would have characteristics similar to those of $b \rightarrow s\gamma$, in particular effective quasi two-body kinematics leading to a hard ϕ momentum spectrum and a small effective mass of the recoiling hadronic system (X_s). Using the analysis method previously applied to measure inclusive $B \rightarrow X_s\gamma$ decays, CLEO-II finds no evidence for $B \rightarrow X_s\phi$ decays with the present data sample and sets an upper limit on the branching ratio of $< 1.1 \times 10^{-4}$ (90% C.L.) for $M(X_s) < 2$ GeV. Using recent predictions of Deshpande et al.²³ the limit can be extrapolated to the total rate: $Br(b \rightarrow s\phi) < 1.3 \times 10^{-4}$ (90% C.L.). This result is consistent with the theoretical predictions by Deshpande and He,²² and excludes half of the predicted range: $(0.6 - 2.0) \times 10^{-4}$.

2.4. Search for electroweak penguin decays

The process $b \rightarrow sl^+l^-$ ($l = e$ or μ) can occur via electroweak penguin or box diagrams. Experiments searched for these decays in the exclusive modes $B \rightarrow Kl^+l^-$ and $B \rightarrow K^*l^+l^-$. In addition to earlier UA1²⁴ and CLEO-II²⁵ results, there are updated results presented by CDF.²⁶ The experiments at hadronic colliders are competitive in this channel with CLEO-II because of high b production rates and manageable backgrounds in dimuon samples, especially after identification of the B decay vertex. The decays $B \rightarrow K^{(*)}J/\psi$, $J/\psi \rightarrow l^+l^-$ due to $b \rightarrow cW^-$, $W^- \rightarrow \bar{c}s$ and binding of the $c\bar{c}$ pair to J/ψ by long distance strong interactions that have a well measured branching ratio, are used as a normalization mode. The experimental upper limits are an order of magnitude away from the theoretical predictions (that include calculation of K and K^* form factors) as shown in Table 2.

2.5. Search for B meson annihilation

Table 2 also summarizes results and predictions for the annihilation processes.

CDF presents²⁷ a search for B^0 and B_s annihilation to $\mu^+\mu^-$. Even though the analysis is restricted to candidates in the central region ($|y| < 1$) with high transverse momenta ($p_t > 6$ GeV) there are about 10^8 B^0 's and 3×10^7 B_s 's produced in this region in the CDF data sample. CDF sets the first upper limit on $B_s \rightarrow \mu^+\mu^-$ branching fraction and sets the limit on $B^0 \rightarrow \mu^+\mu^-$ rate which is a factor of three more stringent than the CLEO-II results²⁸ based on about 1.6×10^6 B^0 's.

The L3 experiment presents²⁹ the first upper limits on B^0 and B_s annihilation

Table 2. Searches for electroweak penguin decays and for annihilation of B mesons. Upper limits are given at 90% C.L.

	$Br(B^- \rightarrow K^- l^+ l^-)$		$Br(B^0 \rightarrow K^{*0} l^+ l^-)$		
	$e^+ e^-$	$\mu^+ \mu^-$	$e^+ e^-$	$\mu^+ \mu^-$	
S.M.	$0.04 - 0.08 \times 10^{-5}$	$0.04 - 0.08 \times 10^{-5}$	$0.5 - 0.7 \times 10^{-5}$	$0.3 - 0.4 \times 10^{-5}$	
UA1 ²⁴ CLEO-II ²⁵ CDF ²⁶	$< 1.2 \times 10^{-5}$	$< 0.9 \times 10^{-5}$ $< 1.1 \times 10^{-5}$	$< 1.6 \times 10^{-5}$	$< 2.3 \times 10^{-5}$ $< 3.1 \times 10^{-5}$ $< 2.1 \times 10^{-5}$	
	$Br(B^0 \rightarrow l^+ l^-)$		$Br(B_s^0 \rightarrow l^+ l^-)$	$Br(B^0 \rightarrow \gamma\gamma)$	$Br(B_s^0 \rightarrow \gamma\gamma)$
	$e^+ e^-$	$\mu^+ \mu^-$	$\mu^+ \mu^-$		
S.M.	2×10^{-15}	8×10^{-11}	2×10^{-9}	$\sim 10^{-8}$	$\sim 10^{-7}$
UA1 ²⁴ CLEO-II ²⁸ CDF ²⁷ L3 ²⁹	$< 5.9 \times 10^{-6}$	$< 8.3 \times 10^{-6}$ $< 5.9 \times 10^{-6}$ $< 1.6 \times 10^{-6}$	$< 8.4 \times 10^{-6}$	$< 3.8 \times 10^{-5}$	$< 1.1 \times 10^{-4}$
	$Br(B^- \rightarrow l^- \bar{\nu}_l)$			$Br(B^- \rightarrow l^- \bar{\nu}_l \gamma)$	
	e^-	μ^-	τ^-	e^-	μ^-
S.M.	$\sim 10^{-13}$	$\sim 10^{-8}$	$\sim 10^{-5}$	$\sim 10^{-6}$	$\sim 10^{-6}$
CLEO-II ^{30,32} ALEPH ³¹	$< 1.5 \times 10^{-5}$	$< 2.1 \times 10^{-5}$	$< 2.2 \times 10^{-3}$ $< 1.8 \times 10^{-3}$	$< 1.6 \times 10^{-4}$	$< 1.0 \times 10^{-4}$

to two photons.

Upper limits on B^- annihilation to a lepton and a neutrino have been recently published by CLEO-II.³⁰ The most stringent upper limit on the decay to $\tau^- \bar{\nu}_\tau$, which has the smallest helicity suppression, is set by ALEPH.³¹ CLEO-II also presents limits on $B^- \rightarrow \gamma l^- \bar{\nu}_l$, where the emission of a photon removes helicity suppression.³²

All the limits are several orders of magnitudes looser than the values predicted by the Standard Model. Thus these decays are not likely to provide useful constraints on the B decay constant nor on the CKM elements (V_{td} , V_{ts} , and V_{ub} are involved) in the near future. However, these results verify that there are no non-standard couplings in these processes at the present level of sensitivity.

3. Inclusive $b \rightarrow c$ decays.

3.1. Inclusive semileptonic decays, $b \rightarrow cl^- \bar{\nu}_l$ ($l = e$ or μ).

The inclusive semileptonic branching ratio is related to a value of $|V_{cb}|$. It also offers tests of QCD models of inclusive b decays, both leptonic (via its numerator) and non-leptonic (via the denominator). Finally, it is an important engineering number for the extraction of various Z^0 parameters.

All $b \rightarrow cW^-$ decays, hadronic ($W^- \rightarrow q_{dn}\bar{q}_{up}$) and semileptonic ($W^- \rightarrow l^- \bar{\nu}_l$), are sensitive to a value $|V_{cb}|$. The main obstacle in the extraction of $|V_{cb}|$ from the measured branching ratios is the difficulty of estimating strong interaction effects on the decay rate. Semileptonic decays offer a great simplification compared to hadronic decays since no strong interactions are involved in the decay of the virtual W^- and there is no mixing of lepton generations. In exclusive semileptonic decay modes strong interactions still play a crucial role, since a probability for the creation of a specific hadronic state containing the c and spectator quarks must be estimated. For decays summed over all possible hadronic states, the effect of strong interactions drops out in the lowest order, and the inclusive rate directly reflects short distance weak interactions. There are perturbative QCD corrections of the order of α_s to this approximation. The lowest non-perturbative correction appears only in the second order of the expansion in heavy b quark mass. Thus, the inclusive semileptonic branching ratio is particularly suitable for determination of $|V_{cb}|$.

Theoretically, $\Gamma(b \rightarrow cl^- \bar{\nu}_l) = \gamma_c |V_{cb}|^2$, where in the lowest order γ_c can be found from the muon decay width formula replacing the lepton masses with the quark masses. To eliminate the total width from the denominator of the experimental value of the branching fraction, a measured b quark lifetime must be used: $|V_{cb}| = \sqrt{Br(b \rightarrow cl^- \bar{\nu}_l)/(\gamma_c \tau_b)}$. Both experimental quantities in this formula can be measured very precisely due to their inclusive character. The lifetime has been measured by experiments at Z^0 and in $p\bar{p}$ collisions as discussed in the other paper at

this conference.³³ The inclusive semileptonic branching ratio has been measured by the experiments at $\Upsilon(4S)$ and at Z^0 .

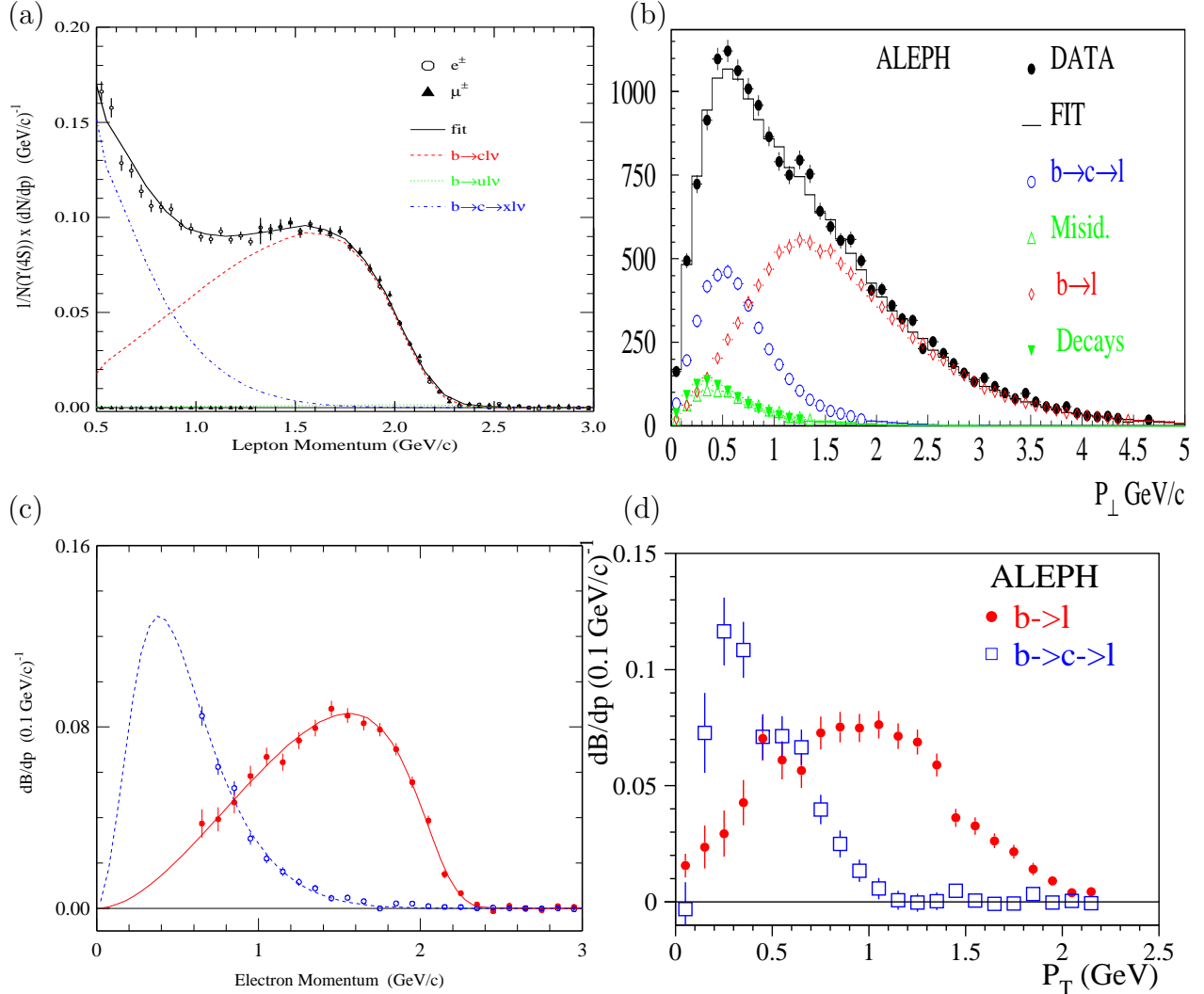


Fig. 6. Inclusive leptons in b decays. (a) Lepton momentum spectrum as measured by CLEO-II at $\Upsilon(4S)$. (b) Spectrum of lepton momentum transverse to the jet direction as measured by ALEPH at Z^0 . (c) Momentum spectra for prompt leptons, $b \rightarrow l$, and cascade leptons, $b \rightarrow c \rightarrow l$, as measured separately in dilepton events by CLEO-II. (d) Transverse momentum spectra for prompt leptons, $b \rightarrow l$, and cascade leptons, $b \rightarrow c \rightarrow l$, as measured separately in dilepton events by ALEPH.

Experimentally $Br(b \rightarrow cl^-\bar{\nu}_l)$ is determined as a ratio of b decays producing a prompt lepton^e, $N_{b \rightarrow l}$, and to all b decays, $N_{b \rightarrow x}$. We will first discuss determination of the denominator. Since non- $B\bar{B}$ decays of $\Upsilon(4S)$ resonance are expected to be very small, threshold experiments calculate $N_{b \rightarrow x}$ by counting multi-track events at and below the $\Upsilon(4S)$ resonance. At the Z^0 peak $N_{b \rightarrow x}$ is equal to a number of hadronic Z^0 decays times $R_{b\bar{b}} \equiv \Gamma_{b\bar{b}}/\Gamma_{had}$. The latter is an interesting quantity by

^eCorrection for prompt leptons from the $b \rightarrow ul^-\bar{\nu}_l$ decays is small.

its own as discussed in the other papers at this conference.³⁴ In a simple approach its value can be set to the world average or to the Standard Model prediction like in the recent L3 analysis.³⁵ Using b quark tagging $N_{b \rightarrow x}$ can be estimated from a ratio of number of single-tag events squared and of double-tag events. When a lepton itself is used to tag $b\bar{b}$ events, $Br(b \rightarrow cl^-\bar{\nu}_l)$ and $R_{b\bar{b}}$ can be both determined from single and dilepton samples, however, their values are strongly anti-correlated. This is the approach taken by most of the previous measurements at LEP.^{36,37} In a recent analysis ALEPH³⁸ uses a secondary vertex to tag $b\bar{b}$ events and presents practically uncorrelated measurement of these quantities.

To determine the nominator, $N_{b \rightarrow l}$, leptons from other sources must be estimated. While backgrounds from decays of the other particles, e.g. $N_{c \rightarrow l}$, can be suppressed with b -tagging, background from cascade decays of the b quark, $N_{b \rightarrow c \rightarrow l}$, are more difficult to eliminate. In the B rest frame the prompt leptons have a harder momentum spectrum than the cascade leptons which allows the discrimination between these two contributions. Experiments at the $\Upsilon(4S)$ operate almost at the B rest frame, thus they directly look at the lepton momentum spectrum. In Z^0 decays, b quarks are produced with a varied momentum that on average is fairly large ($\sim 0.7\frac{m_{Z^0}}{2}$). This washes out the differences in lepton momenta for the prompt and the cascade leptons. Therefore, experiments at Z^0 look in the direction in which the b quarks are not moving, i.e. perpendicularly to their motion which is approximated by the jet direction. The distribution of leptons in P_\perp at Z^0 is very similar to the distribution of leptons in P at $\Upsilon(4S)$, as illustrated in Fig. 6a-b. For $P_{(\perp)} > 1.5$ GeV/c the cascade background is very small. To measure total $b \rightarrow l$ rate, the high momentum yield must be extrapolated to the region dominated by the background. Alternatively the entire momentum range can be fit to unfold the prompt and cascade components. In either case, theoretical models for the $b \rightarrow l$ spectrum must be used. For the most accurate measurements by CLEO-II³⁹ at $\Upsilon(4S)$ and ALEPH³⁸ at Z^0 , the model dependence is the largest source of uncertainty. These two measurements dominate world average values of $Br(b \rightarrow cl^-\bar{\nu}_l)$ at $\Upsilon(4S)$ ⁴⁰, $(10.56 \pm 0.17 \pm 0.33)\%$, and at Z^0 ⁴¹, $(10.89 \pm 0.18 \pm 0.24)\%$. The first error is experimental (statistical and systematic) and the second error is an estimate of the model dependence. The central values of the branching fractions correspond to the choice of the quark level model by Altarelli et al.⁴² to predict the shape of the $b \rightarrow cl^-\bar{\nu}_l$ lepton spectrum. The model dependence was estimated as a difference between the meson level model by Isgur et al.⁴³ and the quark level model.

Model independent measurements can be obtained using a technique developed by the ARGUS experiment that utilizes charge and angular correlations in dilepton events.⁴⁴ Selection of a high momentum lepton tags $b\bar{b}$ events. At $\Upsilon(4S)$, the b quarks are produced almost at rest, thus a lepton from the cascade decay of the same b quark should be approximately acollinear to the tag lepton and can be eliminated by the angular cut. The prompt and the cascade lepton from the other b quark decay can be

distinguished by electric charge. Neglecting $B\bar{B}$ oscillation, the prompt lepton should have an opposite charge to the tag lepton. Since the prompt and the cascade spectra are measured independently (except for small feed-across), the prompt component is measured almost in full momentum range and the model dependence is eliminated. The CLEO-II experiment applied the ARGUS technique to a larger data sample (Fig. 6c). ⁴⁵ An average of these two experiments is $(10.16 \pm 0.38 \pm 0.11)\%$ in good agreement with the model dependent determinations. ALEPH presents an analysis that adopts this technique to the LEP data. ³⁸ Since b quarks produced at Z^0 are fast, the angular correlation is reversed, i.e. the high P_\perp lepton, used as a tag, and the cascade lepton from the decay of the same b quark are collinear (Fig. 6d). As in the case of the CLEO measurement, the model dependence is diminished at the expense of the other errors: $(11.01 \pm 0.36 \pm 0.11)\%$.

The measurements at Z^0 are somewhat larger than at $\Upsilon(4S)$. Since the average b quark lifetime at Z^0 is smaller than at $\Upsilon(4S)$ ³³ (no baryons are produced at $\Upsilon(4S)$) the opposite effect was expected. Decay widths, $\Gamma = Br/\tau$, measured at $\Upsilon(4S)$, ^f $64.8 \pm 1.7 \pm 1.4 \text{ ns}^{-1}$ (the second error expresses the model dependence), and at Z^0 , ^g $70.2 \pm 1.5 \pm 1.5 \text{ ns}^{-1}$, differ by about two standard deviations. Fortunately, this disagreement is small compared to theoretical uncertainties in the γ_c factor: ^{47,46} $42.4 \pm 8 \text{ ps}^{-1}$. Therefore, for $|V_{cb}|$ determination we average the $\Upsilon(4S)$ and Z^0 measurements and cover the disagreement by increasing the experimental error: $\Gamma(b \rightarrow cl^-\bar{\nu}_l) = 67.3 \pm 2.7 \text{ ns}^{-1}$. That leads to:

$$|V_{cb}| = 0.0398 \pm 0.0008(\text{experimental}) \pm 0.0040(\text{theoretical}).$$

Theoretical uncertainties due to higher order perturbative corrections are somewhat controversial at present. Following Neubert ⁴⁶ we used above the conservative estimate. Bigi et al. argue that the theoretical error is a factor of two smaller. ⁴⁸

3.2. Charm counting in bottom decays.

Value of the semileptonic branching ratio measured for B mesons, $(10.4 \pm 0.3)\%$, is low compared to the theoretical predictions that typically give $\geq 12.5\%$. ⁴⁹ It has been recently suggested that lower predictions can be obtained by enhancement of the $b \rightarrow c(\bar{c}s)$ contribution to the total width. ⁵⁰ At the same time the predicted number of charm quarks per b quark decay (n_c) increases. To accommodate the experimental value of the semileptonic branching ratio n_c must be raised from about $n_c = 1.15$

^fFor the best estimate of the semileptonic branching fractions, we averaged the results from single lepton and dilepton samples, $Br(B \rightarrow X_c l^-\bar{\nu}_l)_{\Upsilon(4S)} = (10.37 \pm 0.20 \pm 0.23)\%$. The second error expresses the model dependence. To correct for the lifetime, we used $(\tau_{B^-} + \tau_{B^0})/2 = 1.60 \pm 0.03 \text{ ps}$. ³³

^gWe did not include the model independent measurement by ALEPH because of a strong correlation to their other result that has a smaller overall error. ³⁸ To correct for the lifetime, we used $\tau_b = 1.55 \pm 0.02 \text{ ps}$. ³³

to about 1.30%⁵¹ in contradiction with the most recent measurements of inclusive branching ratios by CLEO-II, $n_c < (1.16 \pm 0.05)$. The contributing measurements are shown in Table 3. Thus, discrepancy between the theory and the experiment remains to be resolved.

Table 3. Inclusive charm branching ratios in B meson decays as measured by CLEO-II. The first two numbers are preliminary.

$B \rightarrow X + \dots$	n_c	Ref.
D^0	0.645 ± 0.031	52
D^+	0.235 ± 0.029	52
D_s	0.121 ± 0.017	53
Λ_c	0.064 ± 0.011	54
Ξ_c^0	0.024 ± 0.013	55
Ξ_c^+	0.015 ± 0.007	55
ψ	$2 \times (0.0080 \pm 0.0008)$	56
ψ'	$2 \times (0.0034 \pm 0.0005)$	56
χ_{c1}	$2 \times (0.0037 \pm 0.0007)$	56
χ_{c2}	$2 \times (0.0025 \pm 0.0010)$	56
η_c	$< 2 \times 0.009$	56
Total	$< 1.16 \pm 0.05$	

3.3. Inclusive semileptonic decays, $b \rightarrow c\tau^-\bar{\nu}_\tau$.

Rate for semileptonic decays to the τ lepton is expected to be smaller than to electron or muon because of the phase space suppression. Since the τ lepton decays to many different channels and produces at least one additional neutrino, this rate is difficult to measure experimentally. The yield of events with large missing energy in a hemisphere defined by the jet direction opposite to the vertex or lepton b tag in Z^0 decays is a sensitive measure of the semileptonic rate for decays to τ 's. There are new measurements of this rate by L3⁵⁷ and OPAL⁵⁸, in addition to previous determinations by L3⁵⁹ and ALEPH.³¹ The world average value, $Br(b \rightarrow c\tau^-\bar{\nu}_\tau) = (2.6 \pm 0.3)\%$, is in good agreement with the Standard Model predictions, 2.3–2.8%.⁶⁰ This agreement can be used to set a lower limit on charged Higgs mass in Two-Higgs-Doublet-Models, $m_{H^-} > 2 \tan \beta$ GeV,³¹ that dominates over the limit obtained from $b \rightarrow s\gamma$ decays for very large values of β (see Sec. 2.1.1).

4. Exclusive semileptonic decays, $B \rightarrow X_c l^- \bar{\nu}_l$, $X_c = D, D^*, D^{**}, \dots$

4.1. Form factors

Unlike for inclusive semileptonic decays, weak and strong interactions cannot be easily separated for exclusive decays. The decay width still carries information about $|V_{cb}|$, $\Gamma(B \rightarrow X l^- \bar{\nu}_l) = \gamma_X |V_{cb}|^2$, but the theoretically predicted width γ_X crucially depends on the effect of the strong interactions which is parametrized into form factors (FF) that are a function of q^2 i.e. four-momentum transfer between the initial and final state mesons, $(P_B^\nu - P_X^\nu)^2$; $\gamma_X = G_F^2 \int_0^{(m_B - m_X)^2} \dots FF(q^2) \dots dq$. The form factors contain information about structure of initial and final state mesons. For decays to pseudo-scalars and negligible lepton mass there is only one form factor, $F_1(q^2)$. Three form factors are involved in decays to vector mesons, $A_1(q^2)$, $A_2(q^2)$, $V(q^2)$. Phenomenological models are used to predict form factors. The models must predict both q^2 dependence and absolute normalization of the form factors. While the q^2 dependence can be eventually verified on the data (large statistics are needed), the normalization must be taken from the models. Therefore, measurements of exclusive semileptonic branching fractions lead to model dependent determinations of $|V_{cb}|$.

4.2. Heavy Quark Effective Theory

In recent years, development of the Heavy Quark Effective Theory allowed overcoming most of the model dependence in extraction of $|V_{cb}|$ from the exclusive semileptonic decays.⁶¹ In the limit of infinitely heavy quark mass, heavy-light mesons behave like single electron atoms. Spin of the heavy quark (“nucleus”) can be to a good approximation neglected. Also, different flavor mesons (“isotopes”) have the same structure when expressed in heavy quark four-velocity, v . In this approximations, B , D and D^* mesons have the same structure and there is only one universal form factor called the Isgur-Wise function⁶², \mathcal{F} , that depends on q^2 via four-velocity transfer, $(v_B - v_X)^2$;

$$\begin{aligned} F_1(q^2) &= \frac{m_B + m_X}{2\sqrt{m_B m_X}} \mathcal{F}(y(q^2)) \\ V(q^2) &= A_2(q^2) = \frac{A_1(q^2)}{1 - q^2/(m_B + m_X)^2} = \frac{m_B + m_X}{2\sqrt{m_B m_X}} \mathcal{F}(y(q^2)) \\ y(q^2) &= \frac{m_B^2 + m_X^2 - q^2}{2m_B m_X} = v_B \cdot v_X \equiv v_b \cdot v_c = 1 - (v_B - v_X)^2/2 \end{aligned}$$

The heavy quark symmetry limit is an approximation to QCD. To make HQET useful in practice, α_s , Λ_{QCD}/m_b , and Λ_{QCD}/m_c corrections must be calculated.

General form of the universal form factor, $\mathcal{F}(y)$, is not predicted by HQET and phenomenological models are still needed for calculation of the total expected rate.

However, at one point at which there is no recoil between the initial and final state mesons, $v_X = v_B$ (i.e. at $y = 1$ or at maximal q^2), the hadronic system is unaffected, and an overlap between B and X wave functions (that are identical) is complete: $\mathcal{F}(1) = 1$. This is a model independent prediction. Measurement of the exclusive decay rate at this particular point allows an almost model independent determination of $|V_{cb}|$.

4.3. Exclusive $B \rightarrow Dl^-\bar{\nu}_l$.

So far the decays $B \rightarrow Dl^-\bar{\nu}_l$ have been studied only at $\Upsilon(4S)$. The main background originates from the other semileptonic decays, $B \rightarrow D^*l^-\bar{\nu}_l$ and $B \rightarrow D^{**}l^-\bar{\nu}_l$. Soft pion from the $D^* \rightarrow \pi D$ decay can easily escape detection. Since the neutrino is also undetected, the main experimental challenge is to distinguish events with a missing neutrino from events in which more particles have been missed. ARGUS⁶³ and CLEO-I.5⁶⁴ used a technique in which the neutrino mass was calculated in an approximate way: $m_\nu^2 = (E_B - E_{Dl})^2 - |\vec{p}_B|^2 - |\vec{p}_{Dl}|^2 + 2|\vec{p}_B||\vec{p}_{Dl}|\cos\theta_{B,Dl} \approx (E_{beam} - E_{Dl})^2 - (E_{beam}^2 - m_B^2) - |\vec{p}_{Dl}|^2$. Neglecting the term with unknown $\theta_{B,Dl}$ angle does not change the mean value of m_ν^2 but adds to the experimental resolution. Within this resolution the $B \rightarrow Dl^-\bar{\nu}_l$ signal peaking at zero overlapped with the background peaks only slightly shifted upwards in the m_ν^2 variable. The fit of the signal and background contributions to the m_ν^2 distribution determined the $B \rightarrow Dl^-\bar{\nu}_l$ branching ratio with rather large errors, especially for $B^- \rightarrow D^0l^-\bar{\nu}_l$ where the D^* background peak was much larger than the signal peak.

Recent CLEO-II analysis⁶⁵ overcomes this background limitation at the expense of statistics by reconstructing neutrino four-momentum: $(E_\nu, \vec{p}_\nu) \approx (2E_{beam} - E_{visible}^{event}, -\vec{p}_{visible}^{event})$. Charge conservation is imposed to eliminate events with unreconstructed charged tracks. To suppress events with more than one neutrino only one lepton in the event is allowed. Cut on neutrino mass, $E_\nu^2 - p_\nu^2$, reduces the background with other unreconstructed particles e.g. K_L^0 . Since the achieved resolution is better for the missing momentum ($\sigma(p_\nu) = 0.11$ GeV/c) than for the missing energy ($\sigma(E_\nu) = 0.26$ GeV) the former is used to impose the beam energy constraint ($E_{Dl} + |\vec{p}_\nu| = E_{beam}$) and to calculate the B meson mass ($M_B = \sqrt{E_{beam}^2 - (\vec{p}_{Dl} + \vec{p}_\nu)^2}$). The D^* background is significantly reduced with this method, thus $Br(B^- \rightarrow D^0l^-\bar{\nu}_l)$ is measured with improved precision.

Averaging the previous ARGUS measurement, $Br(\bar{B}^0 \rightarrow D^+l^-\bar{\nu}) = (2.0 \pm 0.7 \pm 0.5)\%$, and the new CLEO-II measurement, $Br(B^- \rightarrow D^0l^-\bar{\nu}) = (2.0 \pm 0.3 \pm 0.5)\%$, corrected for the B lifetimes^h we obtain: $\Gamma(B \rightarrow Dl^-\bar{\nu}_l) = 12.4 \pm 3.0 \text{ ns}^{-1}$. From several models of form factors⁶⁶ we estimate, $\gamma_D = (8.9 \pm 3.1) \text{ ps}^{-1}$, where the error

^h We used $\tau_{B^-} = 1.62 \pm 0.05 \text{ ps}$ and $\tau_{B^0} = 1.57 \pm 0.05 \text{ ps}$.³³

is the difference between the largest and the smallest prediction. The above leads to,

$$|V_{cb}| = 0.0373 \pm 0.0045 \pm 0.0065$$

where the first error is experimental and the second reflects the model dependence.

Fig. 7 shows q^2 distribution measured for $B^- \rightarrow D^0 l^- \bar{\nu}_l$ by CLEO-II. As expected from the helicity suppression in B decay to a pseudo-scalar, the rate quickly tends to zero when approaching the maximal q^2 value (zero recoil point). At the same time the D^* background increases. This illustrates that the $B^- \rightarrow D^0 l^- \bar{\nu}_l$ channel will be very difficult to use to determine $|V_{cb}|$ in model independent way even for much larger experimental statistics. This channel is also disfavored theoretically as the Λ_{QCD}/m_c correction to the heavy quark symmetry limit does not vanish.

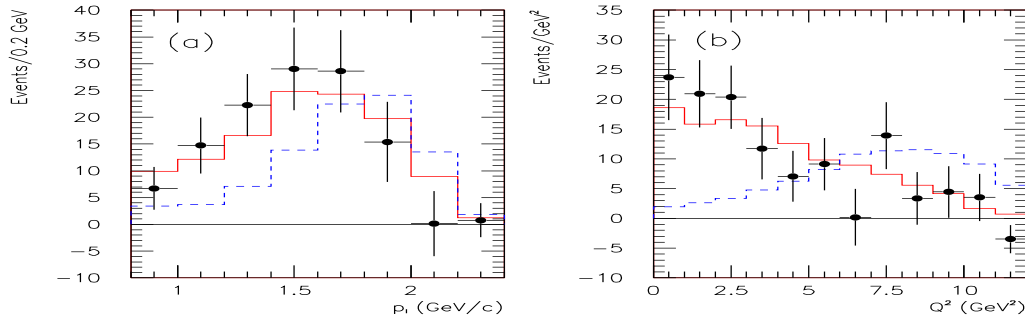


Fig. 7. Lepton momentum (a) and q^2 (b) distributions in $B^- \rightarrow D^0 l^- \bar{\nu}_l$ decays measured by CLEO-II (points with error bars). The data points are not efficiency corrected. The solid curves correspond to the Monte Carlo simulation of the signal, whereas the dashed curves represent the Monte Carlo simulation of the $B \rightarrow D^* l^- \bar{\nu}_l$ background.

4.4. Exclusive $B \rightarrow D^* l^- \bar{\nu}_l$.

4.4.1. Branching ratio and model dependent determination of $|V_{cb}|$.

The technique that uses m_ν^2 determined in the approximate way to extract an exclusive semileptonic branching fraction works better for the D^* channel than for the D channel, since a ratio of the background (D^{**}) to the signal branching ratios is favorable. In a recently published analysis,⁶⁷ CLEO-II modified this technique and used a two-dimensional distribution of m_ν^2 vs. $2 |\vec{p}_B| |\vec{p}_{D^2 l}|$ (the latter is a factor multiplying the unknown $\cos \theta_{B,D^* l}$ term - see Sec. 4.3).

Since a slow pion from the $D^* \rightarrow \pi D$ decay preserves the D^* direction in the laboratory system and its momentum is proportional to the D^* momentum, the entire D^* four-momentum can be approximately reconstructed by detecting the transition pion alone. This method allowed ARGUS⁶⁸ to overcome the statistical limitation of their original measurement.⁶⁹

This year there are two new measurements of the $\bar{B}^0 \rightarrow D^{*0} l^- \bar{\nu}_l$ branching ratio presented by the LEP experiments: ALEPH⁷⁰ and DELPHI.⁷¹ At Z^0 the slow pion is boosted up in momentum into a region of large and uniform detection efficiency. This advantage over the measurements at the $\Upsilon(4S)$ is offset by an additional normalization error from the $Z^0 \rightarrow B^0$ rate and by reconstruction difficulties due to unknown B^0 energy and momentum. The latter has been overcome with help of silicon vertex detectors that are able to determine direction of the B^0 momentum from the separation of the B^0 decay vertex from the interaction point. Neutrino energy is calculated from the missing energy in the $D^* l$ hemisphere: $E_\nu \approx E_{beam} - E_{visible}^{hem}$. These two quantities, together with the four-momentum conservation and the mass constraints allow full reconstruction of the $\bar{B}^0 \rightarrow D^{*0} l^- \bar{\nu}_l$ kinematics.

For most of the branching ratio measurements uncertainty in the D^{**} background is the dominant error. A cut on the neutrino mass is not as effective in suppression of the D^{**} background at Z^0 as it is at $\Upsilon(4S)$. However, vertexing again comes handy. Events with more than one charged pion pointing to the B^0 decay vertex are rejected. The D^{**} background rejection achieved by ALEPH is a factor of 2.5 worse than in the CLEO-II analysis but comparable to the ARGUS results. DELPHI has a higher background partly because the partial reconstruction of D^* 's is used.

Averaged over all determinations, $Br(\bar{B}^0 \rightarrow D^{*+} l^- \bar{\nu}_l) = (4.47 \pm 0.25)\%$,⁷² $Br(B^- \rightarrow D^{*0} l^- \bar{\nu}_l) = (5.13 \pm 0.67)\%$,⁷³ and $\Gamma(B \rightarrow D^* l^- \bar{\nu}_l) = 28.8 \pm 1.7 \text{ ns}^{-1}$. From the model predictions:⁶⁶ $\gamma_{D^*} = 23.6 \pm 8.2 \text{ ps}^{-1}$. Thus,

$$|V_{cb}| = 0.0350 \pm 0.0010 \pm 0.0061$$

where the second error reflects the model dependence.

4.4.2. Rate at zero recoil point and model independent determination of $|V_{cb}|$.

The $B \rightarrow D^* l^- \bar{\nu}_l$ channel is favored for model independent determination of $|V_{cb}|$ both theoretically and experimentally. It has been shown that the first order non-perturbative correction to the heavy quark symmetry limit must be zero.⁷⁴ The second order non-perturbative correction and the first order perturbative correction have been estimated by several authors, $\mathcal{F}(1) = 0.91 \pm 0.04$.⁴⁶ Experimentally, the D^* channel has the largest branching fraction among all exclusive semileptonic decays. Nevertheless, statistics near the zero recoil point is still very limited, thus the experiments use full y range to extrapolate the measured rate to the $y = 1$ point. Within the present statistical errors the data are well described by a linear function, $|V_{cb}| \mathcal{F}(y) = |V_{cb}| \mathcal{F}(1) (1 - \hat{\rho}^2(y - 1))$, where $|V_{cb}| \mathcal{F}(1)$ and $\hat{\rho}^2$ are free parameters. Various formulae were tried by some experiments to evaluate the extrapolation error.

The above method was first used by ARGUS.⁶⁹ CLEO-II recently published results based on much higher statistics and improved event selection.⁶⁷ Also ALEPH⁷⁰ and DELPHI⁷¹ have applied this method and report new results. Systematic effects

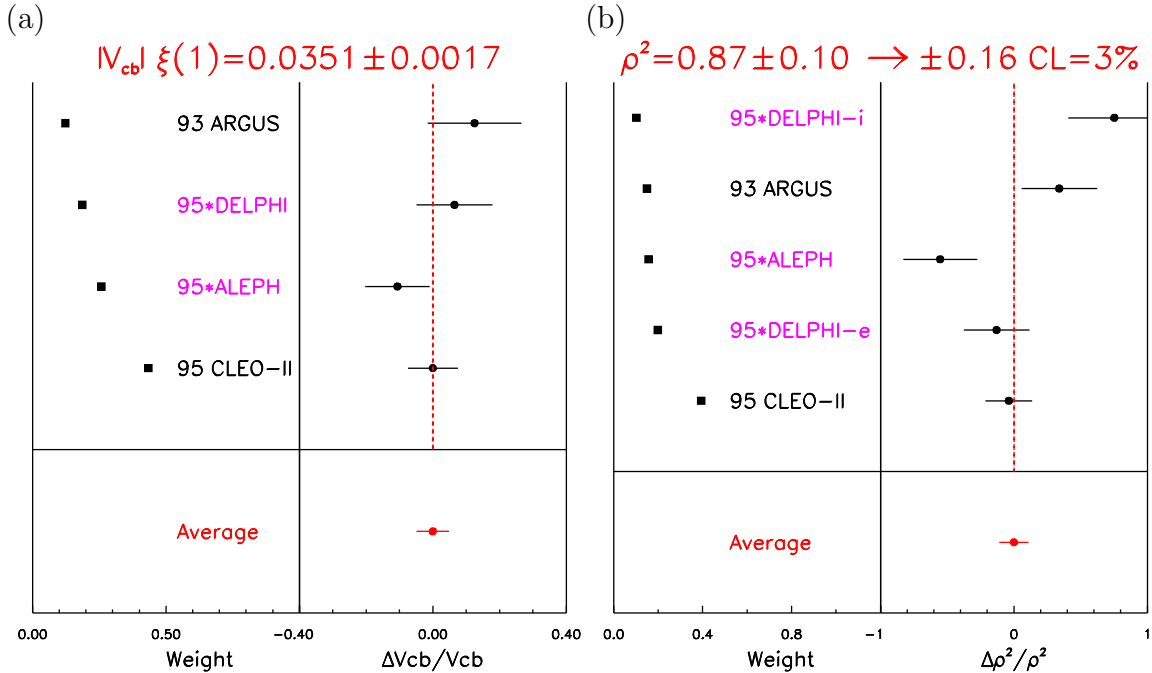


Fig. 8. Comparison of various measurements of: (a) $|V_{cb}| \mathcal{F}(1)$; (b) slope of $\mathcal{F}(y)$. Relative deviations of each measurement from the average value are shown. Weights in which each experiment contributes to the average are also shown. Preliminary measurements are indicated by a star. Two measurements of the slope parameter from DELPHI correspond to the partial (-i) and full (-e) D^* reconstruction methods.

in the measurements at $\Upsilon(4S)$ and at Z^0 are quite different. Thanks to the rest frame kinematics in the $\Upsilon(4S)$ experiments, the y variable is determined by neglecting a small term that depends on θ_{B,D^*} angle, $y = v_B \cdot v_{D^*} = \frac{E_B}{m_B} \frac{E_{D^*}}{m_{D^*}} - \frac{|\vec{p}_B|}{m_B} \frac{|\vec{p}_{D^*}|}{m_{D^*}} \cos \theta_{B,D^*} \approx \frac{E_{D^*}}{m_{D^*}}$. The achieved resolution is about 4% of the total range of y variation. In Z^0 decays, both terms are large and y resolution crucially depends on the measurement of the small θ_{B,D^*} angle with help of silicon vertex detectors. The resolution achieved at LEP is 14-18%. Uncertainties in unfolding the resolution effects becomes the dominant systematics for the DELPHI measurement.

The results are summarized in Fig. 8. While there is a good agreement among all measurement of $|V_{cb}| \mathcal{F}(1)$, probability that all slope measurements are consistent is only 3%. Ignoring this disturbing fact, an average over all experiments gives $|V_{cb}| \mathcal{F}(1) = 0.0351 \pm 0.0017$. This result relies on the assumption that the form factor $\mathcal{F}(y)$ is linear. The effect of using the other functional forms was investigated by ARGUS⁶⁹ and by Stone for the CLEO-II data.⁷⁵ The latter study, based on the higher statistics, shows that the obtained value of $|V_{cb}| \mathcal{F}(1)$ may change up to +4%. The variation is asymmetric because the assumed functions have a positive curvature as expected when approaching a pole. We include this uncertainty in the experimental error:

$$|V_{cb}| = 0.0386^{+0.0025}_{-0.0019} (\text{experimental}) \pm 0.0017 (\text{theoretical}).$$

4.4.3. Tests of the Heavy Quark Effective Theory.

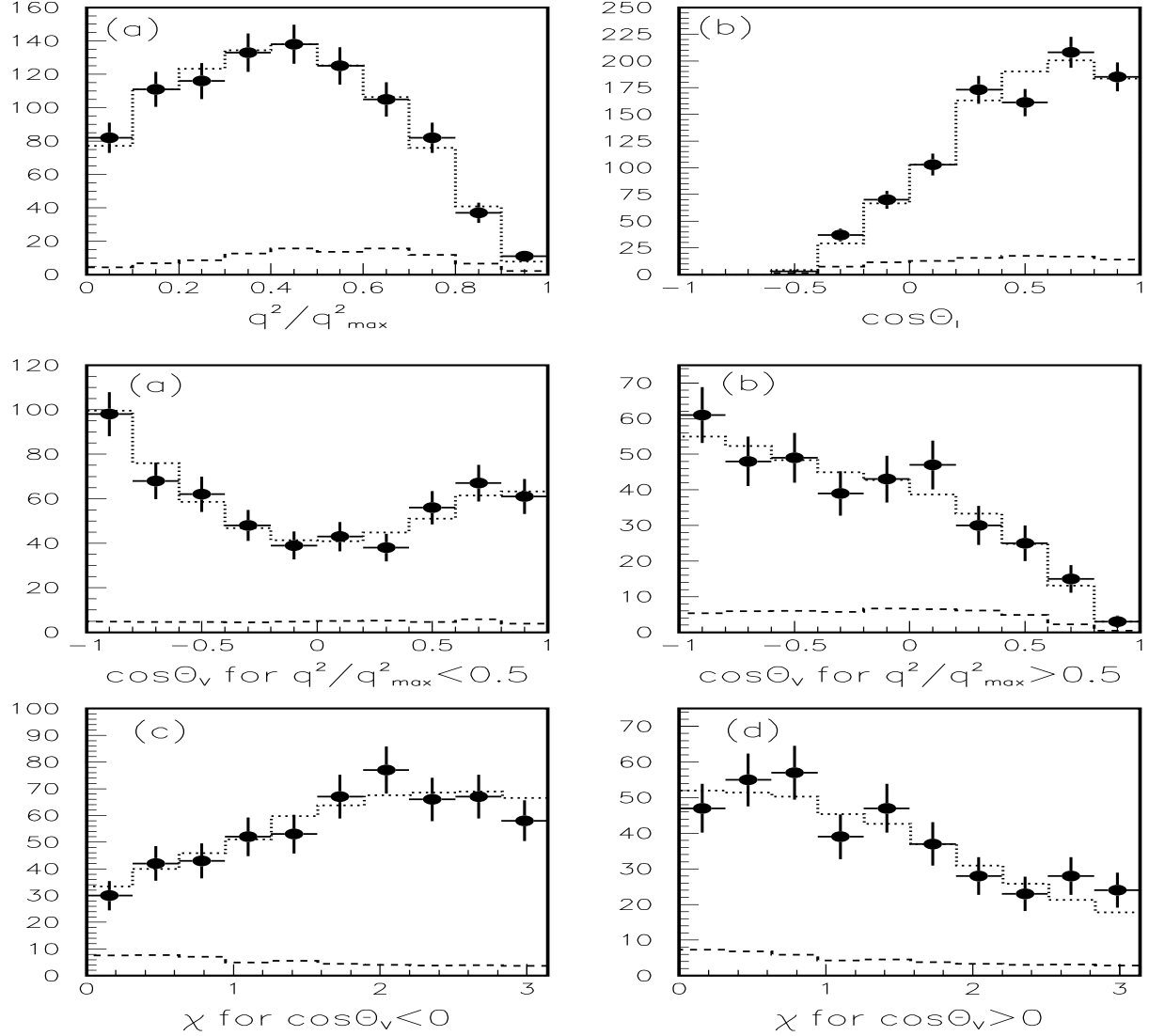


Fig. 9. Distribution of q^2 and various angles (see Ref. 76 for definitions) describing $B \rightarrow D^* l^- \bar{\nu}_l$ decay as measured by CLEO-II. The points with error bars are the data. The dotted histograms show the results of the fit of the HQET motivated form factors. The dashed lines show the estimated backgrounds included in the fit.

Since we rely on HQET for $|V_{cb}|$ determination from the measured rate at the zero recoil point, it is important to test the other prediction of HQET, namely that there should be only one form factor in the heavy quark symmetry limit. Since in the real world this symmetry is broken, it is appropriate to test the modified relation among

the form factors:

$$\frac{V(q^2)}{R_1(y(q^2))} = \frac{A_2(q^2)}{R_2(y(q^2))} = \frac{A_1(q^2)}{1 - q^2/(m_B + m_X)^2} = \frac{m_B + m_X}{2\sqrt{m_B m_X}} h_{A_1}(y(q^2))$$

In the exact symmetry limit, $R_1 = R_2 = 1$, $h_{A_1} = \mathcal{F}$. For the broken symmetry R_1 , R_2 develop mild y dependence and their values at $y = 1$ deviate from unity. The latter is a stronger effect. Also h_{A_1} may differ slightly from the Isgur-Wise function \mathcal{F} .

CLEO-II investigates full four-dimensional correlations in all kinematical variables describing the $B \rightarrow D^* l^- \bar{\nu}_l$ decay.⁷⁶ Since the data statistics are limited, R_1 and R_2 are assumed to be constant and a linear y dependence is assumed for h_{A_1} ($\approx 1 - \rho^2(y - 1)$). As shown in Fig. 9 an excellent fit to the data is obtained. Thus, we conclude that HQET works at the present level of experimental sensitivity. Numerical values obtained for the fitted parameters, $R_1 = 1.18 \pm 0.30 \pm 0.12$, $R_2 = 0.71 \pm 0.22 \pm 0.07$, are in good agreement with the predictions based on broken heavy quark symmetry: $R_1 = 1.15 - 1.35$, $R_2 = 0.79 - 0.91$.⁷⁷ Also the value of the slope parameter, $\rho^2 = 0.91 \pm 0.15 \pm 0.06$, is consistent with the HQET calculations and the results of the fits to the y variable in the $|V_{cb}|$ determinations.⁴⁶

4.5. Semi-exclusive $B \rightarrow D^{**} l^- \bar{\nu}_l$.

Comparison of the measured inclusive semileptonic branching ratio with the exclusively measured branching ratios in decays to D and D^* reveals that about $(35 \pm 7)\%$ of all semileptonic decays must produce higher excitations of the charm mesons, and/or non-resonant states. We have been giving them a generic label of decays to “ D^{**} ” states.

In addition to the two S -wave states ($D - 1^1S_0$, $D^* - 1^3S_1$), four P -wave states are expected (1^1P_1 , 1^3P_0 , 1^3P_1 , 1^3P_2). Experimentally existence of two narrow P states has been established: $D_1(2420)$ (decays to $D^* \pi$) and $D_2^*(2460)$ (decays to $D^* \pi$ and $D \pi$). HQET predicts that the other two states are wide and decay to $D \pi$ and $D^* \pi$ respectively.

First evidence for semileptonic B decays to the D_1^0 state was obtained by the ARGUS experiment.⁶⁹ Ability to correlate soft charged pions with the B decay vertex (same as the D^{**} decay vertex) is a powerful experimental tool available in the Z^0 data. There is a wealth of new information from the LEP experiments. DELPHI⁷⁸ measured decay rate to D_1^0 and D_2^{*0} . ALEPH observes semileptonic decays to the D_1 state in both charge modes.⁷⁹ OPAL⁸⁰ claims the D_2^* signal in both charged modes, but the production of the D_2^{*+} state is not confirmed by ALEPH as illustrated in Fig. 10. CLEO-II⁸¹ sets only upper limits on D_1^0 and D_2^{*0} production but their results are not inconsistent with the LEP measurements. ALEPH also presents evidence for production of wide resonances or non-resonant states in $D^{*+} \pi^-$ and $D^0 \pi^+$.

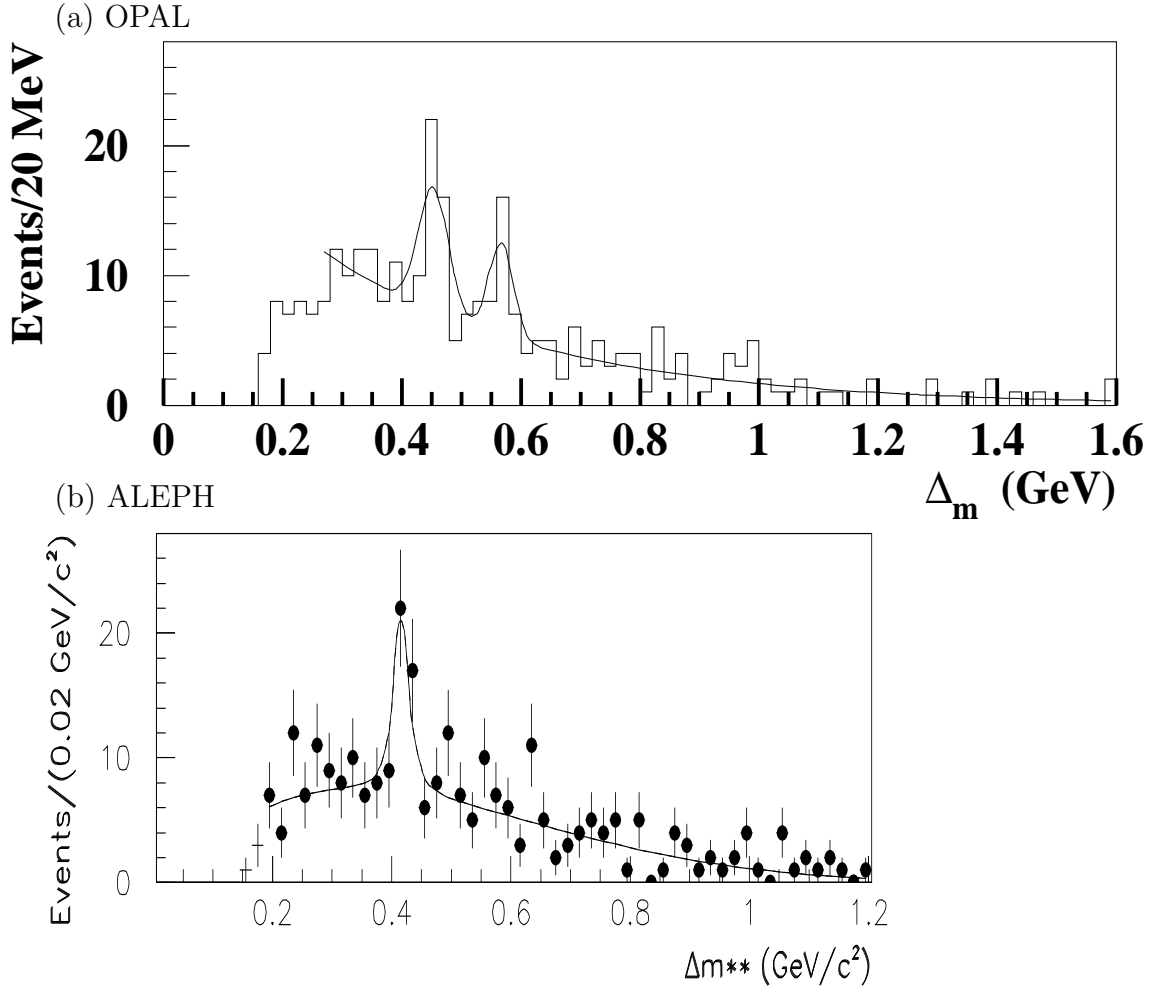


Fig. 10. Mass difference $M(D^0\pi^+) - M(D^0)$ as observed for $B \rightarrow l\bar{\nu}_l D_J^+ X$, $D_J^+ \rightarrow D^0\pi^+$ candidates by OPAL (a) and ALEPH (b). The first peak in the OPAL and ALEPH data is interpreted as a sum of the D_1^+ and D_2^{*+} states decaying to D^{*0} which in turn always decays to $D^0\gamma$ or $D^0\pi^0$ (γ and π^0 are not detected). OPAL measures $Br(B \rightarrow l\bar{\nu}_l D_J^+ X) Br(D_J^+ \rightarrow D^{*0}\pi^+) = (1.8 \pm 0.6)\%$, whereas ALEPH obtains a smaller value, $(0.5 \pm 0.2 \pm 0.1)\%$. OPAL interprets the second peak in their data as evidence for D_2^{*+} production followed by the $D_2^{*+} \rightarrow D^0\pi^+$ decay with a product branching ratio of $Br(B \rightarrow l\bar{\nu}_l D_2^{*+} X) Br(D_2^{*+} \rightarrow D^0\pi^+) = (1.1 \pm 0.3^{+0.2}_{-0.3})\%$. ALEPH finds no evidence for such decays and sets an upper limit of $< 0.2\%$ at 95% C.L. The branching ratios given here assume $f_{B^0} = f_{B^-} = 0.4$ in Z^0 decays.

All of these searches are semi-exclusive i.e. production of other particles in addition to the observed states in the same semileptonic decays is not excluded by the experiments. Consequently the charge of the parent B meson is not determined. Detection efficiency calculated by the experiments depends on the assumptions made about the production mechanism. Furthermore, D_1 and D_2^* decay branching fractions are not known experimentally. All these factors together make interpretation of the experimental results very difficult. We conclude that the experiments confirm production of charm states beyond the D and D^* mesons in semileptonic B decays, but we are still far from quantitative understanding of exclusive branching fractions

in this sector.

5. Summary of $|V_{cb}|$ determinations.

Fig. 11 summarizes all measurements of $|V_{cb}|$ discussed above. The determinations from the inclusive semileptonic rate and from the D^* production rate measured at the zero recoil point agree remarkably well. Even though the determinations from the exclusive semileptonic branching ratios are also consistent, we average only the former two results for the best estimate of $|V_{cb}|$, since the theoretical uncertainties in predictions of the exclusive branching fractions have not been systematically evaluated;

$$|V_{cb}| = 0.0390^{+0.0016}_{-0.0014} \pm 0.0017$$

where the first error is experimental and the second theoretical.

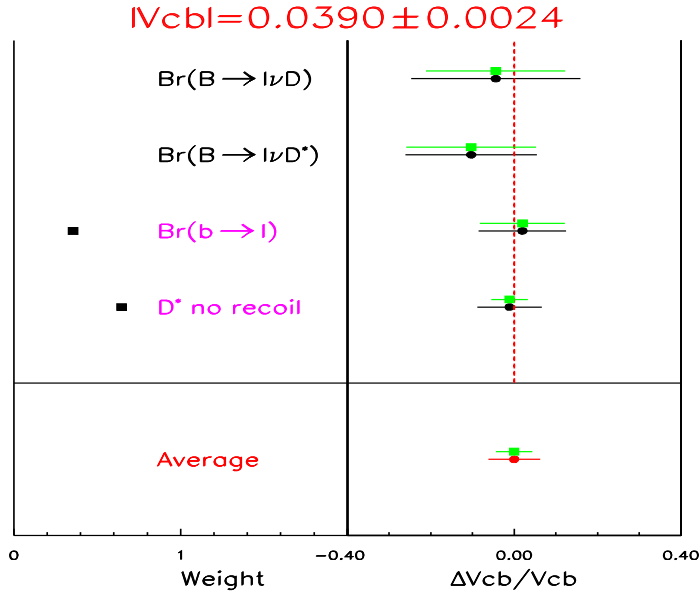


Fig. 11. Comparison of various determinations of $|V_{cb}|$. Relative deviations of each method from the average value are shown. The top errors show theoretical uncertainty alone. The bottom errors show experimental and theoretical errors combined. The determinations from exclusive branching ratios are not used in calculating the average since the theoretical uncertainties in these determinations have not been systematically evaluated. Weights in which the other two methods contribute to the average are also shown.

6. Determination of $|V_{ub}|$.

6.1. Inclusive semileptonic decays, $b \rightarrow u \ell^- \bar{\nu}_\ell$.

The rate for inclusive semileptonic decays of the b quark to the u quark is by

two orders of magnitude smaller than for decays to the c quark. Inclusive $b \rightarrow ul^-\bar{\nu}_l$ decays are very difficult to observe except for the endpoint of the lepton momentum spectrum that extends above the kinematic limit in the $b \rightarrow cl^-\bar{\nu}_l$ decays (due to $m_u \ll m_c$). These decays were first observed by CLEO-I.5⁸² and confirmed by ARGUS⁸³, and later they were measured with a higher precision by CLEO-II.⁸⁴ Unfortunately, determination of $|V_{ub}|$ from these measurements suffers from a large extrapolation factor from the endpoint rate to a total branching ratio that is not well predicted theoretically:⁸⁴

$$\frac{|V_{ub}|}{|V_{cb}|} = 0.08 \pm 0.01 \pm 0.02$$

The first error is experimental, the second reflects the model dependence in the extrapolation factor. Model dependence is large because the form factors in $b \rightarrow u$ decays must be predicted over a much larger range of q^2 than in the $b \rightarrow c$ decays. Different models disagree even on the relative contributions of various exclusive modes to the endpoint region; the predicted ratio of rates for $B \rightarrow \rho l^-\bar{\nu}_l$ and $B \rightarrow \pi l^-\bar{\nu}_l$ decays varies from 1.5⁸⁵ to 4.6.⁸⁶ It has been also suggested that non-resonant $\pi\pi$ production could significantly contribute to the endpoint region.⁸⁷ Experimental information on dynamics of $b \rightarrow ul^-\bar{\nu}_l$ decays is needed to make progress in determining $|V_{ub}|$.

6.2. Exclusive semileptonic decays, $B \rightarrow (\pi, \rho, \omega)l^-\bar{\nu}_l$.

CLEO-II presents⁸⁸ the first observation of exclusive semileptonic decays $B \rightarrow (\pi, \rho, \omega)l^-\bar{\nu}_l$. Previously, the most sensitive search for these decays reported only upper limits.⁸⁹ Suppression of $b \rightarrow cl^-\bar{\nu}_l$ and continuum backgrounds has been improved by reconstruction of the neutrino four-vector from missing energy and momentum in the event. This method has been already outlined in Sec. 4.3. Thanks to the smaller $b \rightarrow c$ background, the lepton momentum range is extended below the endpoint region. As in any reconstruction of exclusive B decays at $\Upsilon(4S)$, the beam energy constraint and the beam constrained B mass are essential tools in signal extraction. For signal events, $\delta E = E_{beam} - (E_{X_u} + E_l + |\vec{p}_\nu|)$ peaks at zero, and $M_B = \sqrt{E_{beam}^2 - (\vec{p}_{X_u} + \vec{p}_l + \vec{p}_\nu)^2}$ peaks at the true B meson mass ($X_u = \pi$, ρ , or ω). Background events populate a wide range in these variables. Two dimensional distributions, ΔE vs M_B , are fit to unfold the signal from the backgrounds. Because the signal branching ratios are small and the neutrino reconstruction technique is costly in detection efficiency (efficiency is a few percent per decay mode) CLEO-II groups the signal channels into pseudo-scalar and vector modes using isospin symmetry: $\frac{1}{2}\Gamma(\bar{B}^0 \rightarrow \pi^+ l^-\bar{\nu}) = \Gamma(B^- \rightarrow \pi^0 l^-\bar{\nu})$, $\frac{1}{2}\Gamma(\bar{B}^0 \rightarrow \rho^+ l^-\bar{\nu}) = \Gamma(B^- \rightarrow \rho^0 l^-\bar{\nu}) \approx \Gamma(B^- \rightarrow \omega l^-\bar{\nu})$. All five decay modes are fit simultaneously. The signal shape in the ΔE , M_B plane is taken from the Monte Carlo simulation. Thus, there are two

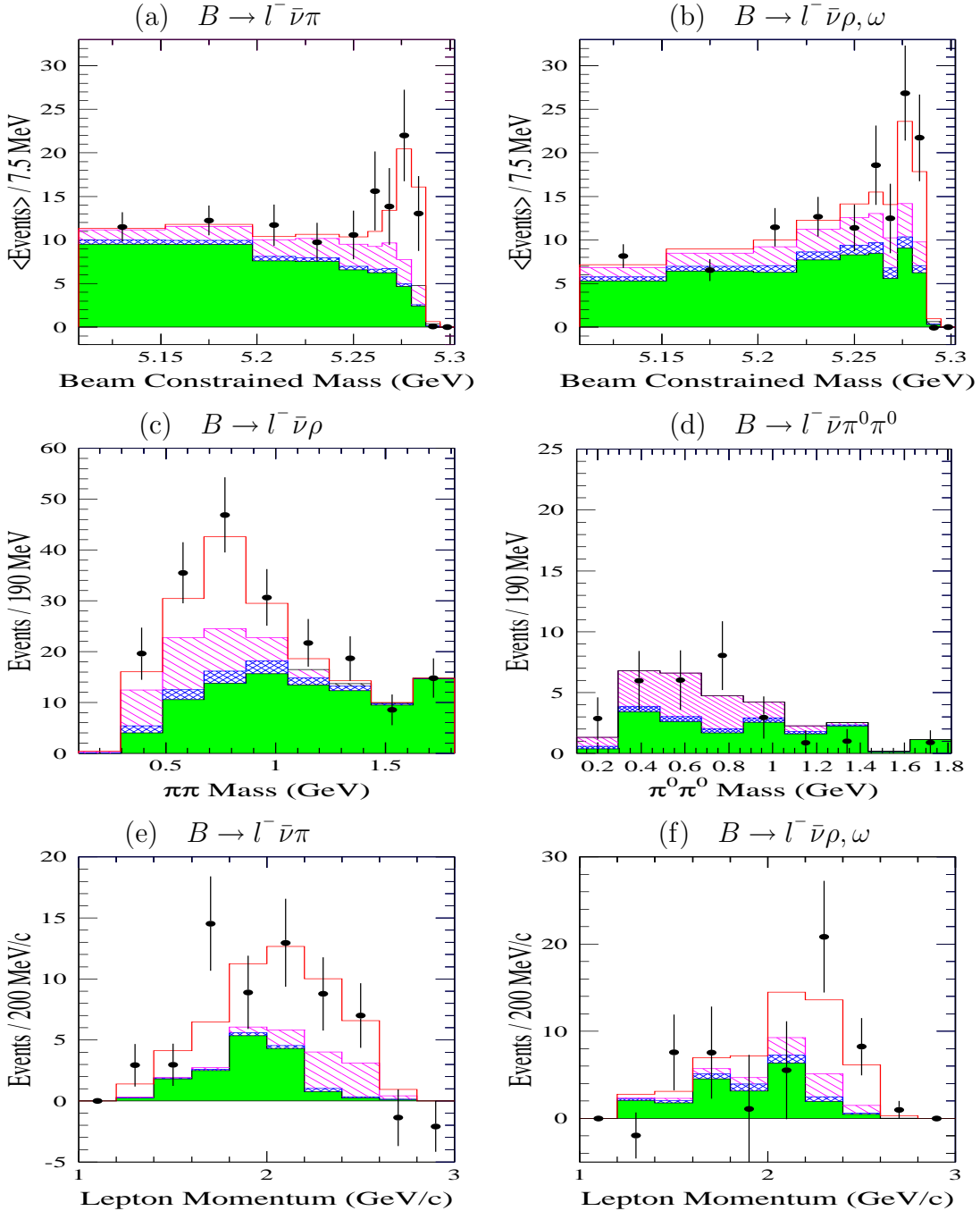


Fig. 12. The data and the projections of the fit in the CLEO-II analysis of exclusive $B \rightarrow (\pi, \rho, \omega) l^- \bar{\nu}_l$ decays. The points are continuum subtracted data. The histograms show the contributions from $b \rightarrow cl^- \bar{\nu}_l$ (shaded), feed-down from higher mass $b \rightarrow ul^- \bar{\nu}_l$ (cross-hatched), signal mode cross-feed (hatched) and signal (hollow). (a),(b) Significant peaks are observed at the B meson mass. (c),(d) Decays to the ρ resonance are observed with no evidence for non-resonant production of $\pi\pi$ states. (e),(f) As expected, lepton momentum spectrum is harder in decays to the vector states.

free parameters in the fit related to the signal branching fractions. The largest background comes from $b \rightarrow cl^-\bar{\nu}_l$ decays (e.g. with undetected K_L^0 or second ν). The shape of this background is fixed from the Monte Carlo simulation and the rate is a free parameter in the fit (alternatively five free parameters are used allowing different scale factors in each mode). Continuum background is small and is subtracted using the data taken below the $\Upsilon(4S)$ resonance. Feed-across between the signal modes is large and is predicted by the Monte Carlo with the scale fixed by the signal parameters. Feed-down from higher mass $b \rightarrow ul^-\bar{\nu}_l$ decay modes is small and it is estimated from the inclusive endpoint analysis with help of the Monte Carlo. Projections of this fit onto several variables of interest are shown in Fig. 12. Significant signals are observed for both pseudo-scalar and vector decay modes (3.9 and 6.4 standard deviations respectively). Presence of the ρ resonance is evident (Fig. 12c) and the results for ω are consistent with the scaling from the ρ channels. No excess of events over the background estimates is seen in the $\pi^0\pi^0$ channel that would have been evidence for non-resonant production (Fig. 12d). Since the detection efficiency is model dependent, CLEO-II presents branching fraction results for various models. The measured branching fractions are consistent with the model predictions and the $|V_{ub}|$ extracted from the inclusive data as shown in Table 4. Both the experimental errors and the model dependence are large. Nevertheless, this measurement constitutes an important milestone in the quest for better determination of $|V_{ub}|$. With increased experimental statistics exclusive reconstructions of semileptonic $b \rightarrow u$ decays will shed light onto strong dynamics of these decays, and consequently help develop more reliable models of inclusive decays.

Table 4. Branching ratios for exclusive $b \rightarrow ul^-\bar{\nu}_l$ decays measured by CLEO-II compared to the model predictions. The uncertainty on $Br(B^0 \rightarrow \rho^-l^+\nu)$ due to possible non-resonant background, $^{+0}_{-20}\%$, is not included below. The model predictions are normalized by assuming $|V_{ub}|/|V_{cb}| = 0.08$ as indicated by the inclusive measurement. The experimental branching ratios are model dependent via the reconstruction efficiency.

Model	$Br(B^0 \rightarrow \pi^-l^+\nu)$		$Br(B^0 \rightarrow \rho^-l^+\nu)$		$Br(\rho^-)/Br(\pi^-)$	
	measured 10^{-4}	predicted 10^{-4}	measured 10^{-4}	predicted 10^{-4}	measured	predicted
ISGW ⁴³	1.3 ± 0.4	0.3	2.3 ± 0.7	1.3	$1.7^{+1.0}_{-0.8}$	4.0
ISGW2 ⁸⁵	2.0 ± 0.7	1.5	3.2 ± 0.9	2.2	$1.6^{+0.9}_{-0.7}$	1.5
KS ⁸⁶	1.6 ± 0.5	1.1	2.7 ± 0.8	5.1	$1.7^{+1.0}_{-0.7}$	4.6
WSB ⁹⁰	1.6 ± 0.6	$1.0 - 1.6$	3.9 ± 1.1	$2.9 - 6.6$	$2.4^{+1.4}_{-1.1}$	$3.0 - 4.3$

7. Conclusions

Decays of the b quark play a unique role for physics of the Cabibbo-Kobayashi-Maskawa matrix. This is also an important place to test our understanding of interplay between strong and weak interactions. Higher order decays of the b quark are also a sensitive window for physics beyond the Standard Model.

Studies of the most common semileptonic $b \rightarrow c$ decays is a mature field both theoretically and experimentally. Measurements of $B \rightarrow D^* l^- \bar{\nu}_l$ rate at zero recoil point by CLEO-II, together with two new measurements by ALEPH and DELPHI at LEP dominate the world average value of $|V_{cb}|$. Even though $|V_{cb}|$ is one of the better known elements of the CKM matrix, impact on the matrix unitarity tests motivates the push for even better determinations of $|V_{cb}|$ in the future.

The process of understanding strong dynamics in semileptonic $b \rightarrow u$ decays have just started with the first observation of the exclusive decay modes by CLEO-II. Eventually this will lead to a better determination of $|V_{ub}|$.

Higher order $b \rightarrow t \rightarrow s$ decays have been observed by CLEO-II via $b \rightarrow s\gamma$ decays. This establishes existence of processes mediated by the penguin diagrams in an unambiguous way. These measurements also provided first direct results for $|V_{ts}|$ and plentiful constraints on extensions of the Standard Model. In addition to increased experimental statistics, next-to-leading order theoretical calculations are needed for better constraints in the future. Siblings of the electromagnetic penguin, gluonic and electroweak penguins, should be experimentally established in the next few years.

Similar $b \rightarrow t \rightarrow d$ decays, that would provide a measurement of $|V_{td}|$, have not been yet observed. These decays will be in the detection range of the next generation of b experiments at e^+e^- colliders already under construction.

Studies of b decays, together with $B\bar{B}$ oscillations and CP-violations, which are discussed in separate papers at this conference, are a dynamic experimental field. In addition to the upgraded CLEO experiment (CLEO-III), two new asymmetric e^+e^- colliders are under construction at KEK and SLAC with the main goal of detecting the CP violation in b decays. Enormous exploratory potential also exists at machines with high energy hadronic beams. HERA-B experiment is under construction at DESY. Hopefully Tevatron and LHC will also exercise in full their reach in b quark physics.

8. Acknowledgements

I would like to thank the people who provided me with the information on recent experimental results, in particular: Chafik Benchouk, Concezio Bozzi, Roger Forty, Pascal Perret and Vivek Sharma from ALEPH, Ronald Waldi from ARGUS, Fritz Dejongh from CDF, Bob Clare and David Stickland from L3, Wilbur Venus from DEL-

PHI, Andrzej Zieminski from D0, Chris Hawkes and Bob Kowalewski from OPAL, Marina Artuso, Ken Bloom, Lawrence Gibbons, Klaus Honscheid, Chris Jones, Suzanne Jones, Scott Menary, Giancarlo Moneti, Hitoshi Yamamoto and the other colleagues from CLEO. I would also like to thank Matthias Neubert and Joe Kroll for useful exchange of information. Last but not least, I would like to thank Sheldon Stone for valuable suggestions concerning this article.

9. References

1. S.L. Wu; P. Franzini; E. Paschos, invited papers contributed to *this conference*.
2. See e.g. L. Littenberg, G. Valencia *Annu. Rev. Nucl. Part. Sci.* **43** (1993) 729.
3. G. Eliam, A. Ioannissian, R.R. Mendel, P. Singer, Preprint *TECHNION-PH* 95-18, *hep/ph* 9507267 (1995); N.G. Deshpande, X.-G. He, J. Trampetic, Preprint *OTIS*-564-REV, *hep/ph* 9412222 (1994).
4. R. Ammar *et al.*(CLEO-II), *Phys. Rev. Lett.* **71** (1993) 674.
5. K.W. Edwards *et al.* (CLEO-II), Paper contributed to *this conference* and to the *EPS Conference, Brussels* (1995) No.0160.
6. M.S. Alam *et al.* (CLEO-II), *Phys. Rev. Lett.* **74** (1995) 2885.
7. The DELPHI collaboration, Paper contributed to *this conference* and to the *EPS Conference, Brussels* (1995) No.0567.
8. A. Ali, C. Greub, Preprint *DESY* 95-117, *SLAC-PUB* 95-6940.
9. R.D. Dikeman, M. Shifman, N.G. Uraltsev, Preprint *TPI-MINN* 95-9-T, *it hep-ph/9505397*, Paper contributed to *this conference* and to the *EPS Conference, Brussels* (1995) No.0741; A. Kapustin, Z. Ligeti, *Phys. Lett.* **B355** (1995) 318.
10. J. O'Donnell, *Phys. Lett.* **B175** (1986) 3691 [97%]; N.G. Deshpande *et al.*, *Phys. Rev. Lett.* **59** (1987) 183 [6%]; C.A. Dominguez *et al.*, *Phys. Lett.* **B214** (1988) 459 [28 \pm 11%]; T. Altomari, *Phys. Rev. D* **37**, (1988) 3 [4.5%]; N.G. Deshpande J. Trampetic, *Mod. Phys. Lett.* **A4** (1989) 2095 [6 – 14%]; T.M. Aliev *et al.*, *Phys. Lett.* **B237** (1990) 569 [39%]; A. Ali, T. Mannel, *Phys. Lett.* **B264** (1991) 447, **B274** (1992) 526 (E) [28 – 40%]; R.N. Faustov, V.O. Galkin, *Mod. Phys. Lett.* **A7** (1992) 2111 [6.5%]; A. Ali, T. Ohl, T. Mannel, *Phys. Rev.* **298B** (1993) 195 [3.5 – 12.2%]; E. El-Hassan, Riazuddin, *Phys. Rev.* **D47** (1993) 1026 [0.7 – 12%]; J. O'Donnell, H.K. Tung, *Phys. Rev. D* **48** (1993) 2145 [10%]; P. Ball, Preprint *TUM-T31-43/93*, *hep/ph* 9308244 (1993) [20 \pm 6%]; A. Ali, C. Greub, *Phys. Lett.* **B259** (1991) 182 [13 \pm 3%]; A. Ali, V.M. Braun, H. Simma, *Z. Phys.* **C63** (1994) 437 [16 \pm 5%]; C. Bernard, P. Hsieh, A. Soni, *Phys. Rev. Lett.* **72** (1994) 1402 [6.0 \pm 1.1 \pm 3.4%]; S. Narison, *Phys. Lett.* **B327** (1994) 354 [15 \pm 4%]; K.C. Bowler *et al.*(UKQCD Collaboration),

Preprint *Edinburgh* 94/544, *hep/lat*9407013 (1994) [$9 \pm 3 \pm 3 \pm 1\%$]; D. Atwood, A. Soni, *Z. Phys.* **C64** (1994) 241 [1.6 – 2.5%]; M. Ciuchini, E. Franco, G. Martinelli, L. Reina, L. Silvestrini *Phys. Lett.* **B334** (1994) 137 [23 \pm 9%]. The numbers in the square brackets are the predictions for the R_{K^*} ratio to be compared with the experimental value $19 \pm 6 \pm 4\%$.

11. A. Buras *et al.*, *Nucl. Phys.* **B424** (1994) 374.
12. See e.g. J. Hewett, Preprints *SLAC-PUB* 94-6521; 95-6782 and references therein.
13. M. Athanas *et al.* (CLEO-II), Paper contributed to *the XXVII Int. Conf. on High Energy Phys. Glasgow*, (1994) No.0159.
14. A. Ali, V.M. Braun, H. Simma, *Z. Phys.* **C6** (1994) 437.
15. D. Attwood, B. Blok, A. Soni Preprint *TECHNION-PH* 94-11, *SLAC-PUB* 95-6635(1994), *hep/ph* 9408373; N.G. Deshpande, X.-G. He, J. Trampetic, Preprint *OTIS-564-REV*, *hep/ph* 9412222 (1994); H.-Y. Cheng, Preprint *IP-ASTP-23-94*, *hep/ph* 9411330 (1994); J.M. Soares, Preprint *TRI-PP-95-6*, *hep/ph* 9503285 (1994); J. Milana, Preprint *UMD-PP-95-110*, *hep/ph* 9503376 (1995); G. Ricciardi, *Phys. Lett.* **B355** (1995) 313; A. Khodzhamirian, G. Stoll, D. Wyler *Phys. Lett.* **B358** (1995) 129; A. Ali, V.M. Braun, *Phys. Lett.* **B359** (1995) 223.
16. For a recent review see S. Playfer, S. Stone, Preprint *HEPSY* 95-01, *hep/ph* 9505392 (1995).
17. M. Battle *et al.* (CLEO-II), *Phys. Rev. Lett.* **71** (1993) 3922.
18. D.M. Asner *et al.* (CLEO-II), Paper contributed to *this conference* and to the *EPS Conference, Brussels* (1995) No.0161.
19. The ALEPH collaboration, Paper contributed to *this conference* and to the *EPS Conference, Brussels* (1995) No.0399.
20. The L3 collaboration, Paper contributed to *this conference* and to the *EPS Conference, Brussels* (1995) No.0093-1.
21. R. Akers *et al.* (OPAL), *Phys. Lett.* **B337** (1994) 393.
22. N.G. Deshpande, Xiao-Gang He, *Phys. Lett.* **B336** (1994) 471; Proceedings of *the XXVII Int. Conf. on High Energy Phys. Glasgow*, Eds. P.J. Bussey and I.G.Knowles, Institute of Physics Publishing (1994), p. 1311.
23. N.G.Deshpande, G. Eilam, Xiao-Gang He, Josip Trampetic, Preprint *OITS-575*, *TECHNION-PH-95-12*, (1995).
24. Albajar *et al.* (UA1), *Phys. Lett.* **B262** (1991) 163.
25. R. Balest *et al.* (CLEO-II), Paper contributed to *the XXVII Int. Conf. on High Energy Phys. Glasgow*, (1994) No.0389.
26. The CDF Collaboration, paper contributed to *this conference*, *Fermilab-Conf 95/201-E* (1995).
27. The CDF Collaboration, paper contributed to *this conference*, *Fermilab-Conf 95/229-E* (1995).

28. R. Ammar *et al.*, *Phys. Rev.* **D49** (1994) 5701.
29. The L3 collaboration, Paper contributed to *this conference* and to the *EPS Conference, Brussels* (1995) No.0093-2.
30. M. Artuso *et al.* (CLEO-II), *Phys. Rev. Lett.* **75** (1995) 785.
31. D. Buskulic *et al.* (ALEPH) *Phys. Lett.* **B343** (1994) 444.
32. R. Balest *et al.*(CLEO-II), Paper contributed to *this conference* and to the *EPS Conference, Brussels* (1995) No.0163.
33. J. Kroll, invited paper contributed to *this conference*.
34. P. Renton, invited paper contributed to *this conference*.
35. The L3 collaboration, Paper contributed to *this conference* and to the *EPS Conference, Brussels* (1995) No.0112.
36. R. Akers *et al.* (OPAL), *Z. Phys.* **C60** (1993) 199.
37. P. Abreu *et al.* (DELPHI), *Z. Phys.* **C66** (1995) 323.
38. The ALEPH collaboration, Paper contributed to *this conference* and to the *EPS Conference, Brussels* (1995) No.0404.
39. J. Bartelt *et al.* (CLEO-II), *CLEO-CONF* 93-19, Paper contributed to *the XVI International Symposium on Lepton and Photon Interactions, Ithaca, NY, (1993)*.
40. The following results were averaged: [4%] K. Wachs *et al.*(Crystal Ball), *Z. Phys.* **C42** (1989) 33; [10%] H. Albrecht *et al.*(ARGUS), *Phys. Lett.* **B249** (1990) 359; [12%] C. Yanagisawa *et al.*(CUSB-II), *Phys. Rev. Lett.* **66** (1991) 2436; [15%] S. Henderson *et al.*(CLEO-I.5), *Phys. Rev. D45*, (1992) 2212; and [59%] Ref. 39 (CLEO-II) (1993). The numbers in square brackets specify weights assigned to each measurement. Some results were corrected to express model dependence in a uniform way as described in the text.
41. The following results were averaged: [6%] Ref. 36 (OPAL) (1993); [20%] Ref. 37 (DELPHI) (1995); [17%] Ref. 35 (L3) (1995); [58%] Ref. 38 (ALEPH) (1995). The numbers in square brackets specify weights assigned to each measurement. Some results were corrected to express model dependence in a uniform way as described in the text.
42. G. Altarelli, N. Cabibbo, G. Corbo, L. Maiani, *Nucl. Phys.* **B208** (1982) 365.
43. N. Isgur, D. Scora, B. Grinstein, M. B. Wise, *Phys. Rev.* **D39** (1989) 799, N. Isgur, M. B. Wise, *Phys. Lett.* **B232** (1989) 113, **B237** (1990) 527. This model is often modified by increasing amount of D^{**} production to better describe the data.
44. H. Albrecht *et al.* (ARGUS), *Phys. Lett.* **B318** (1993) 397.
45. B. Barish *et al.* (CLEO-II), Preprint *CLNS 95/1362 CLEO 95-17* (1995).
46. M. Neubert, invited paper contributed to *this conference*.
47. P. Ball, M. Beneke, V.M. Braun, *Phys. Rev.* **D52** (1995) 3929. The error assigned corresponds to the theoretical uncertainties as discussed by Neubert at *this conference*. See also: M. Luke, M.J. Savage, *Phys. Lett.*, **B321** (1994)

- 88; and Ref. 48.
48. I.I. Bigi, Preprint *UND-HEP* 95-BIG06, *hep/ph* 9507364 (1995); M. Shifman, N.G. Uraltsev, Preprint *TPI-MINN* 94/41-T *hep/ph* 9412398; M. Shifman, N.G. Uraltsev, A. Vainshtein, *Phys. Rev.* **D45** (1995) 2217.
 49. I. Bigi, B. Blok, M.A. Shifman, A. Vainshtein, *Phys. Lett.* **B323** (1994) 408.
 50. A.F. Falk, M.B. Wise, I. Dunietz, *Phys. Rev.* **D51** (1995) 1183; E. Bagan, P. Ball, V.M. Braun, P. Godzinsky, *Phys. Lett.* **B342** (1995) 362; M.B. Voloshin, *Phys. Rev.* **D51** (1995) 3948. More detailed discussion of recent theoretical developments can be found in Ref. 46.
 51. G. Buchalla, I. Dunietz, H. Yamamoto, Preprint *FERMILAB-PUB* 95-167-T, *hep/ph* 9507437 (1995).
 52. The CLEO collaboration, private communication. See also T. Browder (CLEO-II) in the Proceedings of the *Int. Europhys. Conf. on High Energy Phys.* **Brussels** (1995).
 53. D. Gibaut *et al.* (CLEO-II), Preprint *CLNS* 95/1354 (1995).
 54. G. Crawford *et al.* (CLEO-II), *Phys. Rev.* **D45** (1992) 752.
 55. D. Cinabro *et al.* (CLEO-II), Paper contributed to the *XXVII Int. Conf. on High Energy Phys.* **Glasgow**, (1994) No.0865.
 56. R. Balest *et al.* (CLEO-II), *Phys. Rev.* **D52** (1995) 2661.
 57. The L3 collaboration, Paper contributed to *this conference* and to the *EPS Conference, Brussels* (1995) No.0112.
 58. The OPAL collaboration, Paper contributed to *this conference* and to the *EPS Conference, Brussels* (1995) No.0282.
 59. B. Adeva *et al.* (L3), *Phys. Lett.* **B332** (1994) 201.
 60. P. Heiliger, L.M. Sehgal, *Phys. Lett.* **B229** (1989) 409; A.F. Falk, Z. Ligeti, M. Neubert, Y. Nir, *Phys. Lett.* **B326** (1994) 145.
 61. See e.g. M. Neubert, *Phys. Rep.* **245** (1994) 259 and references therein.
 62. N. Isgur, M.B. Wise, *Phys. Lett.* **B232** (1989) 113, **B237** (1990) 527.
 63. H. Albrecht *et al.* (ARGUS), *Phys. Lett.* **B229** (1989) 175.
 64. R. Fulton *et al.* (CLEO-I.5), *Phys. Rev.* **D43** (1991) 651.
 65. Y. Kubota *et al.* (CLEO-II), Paper contributed to *this conference* and to the *EPS Conference, Brussels* (1995) No.0166.
 66. The central values of γ_D and γ_{D^*} correspond to the average over the following model predictions: Ref. 43; Ref. 86; Ref. 90; W. Jaus, *Phys. Rev.* **D41** (1990) 3394. The γ_D error is estimated as the difference between the maximal and the minimal predicted value. The γ_{D^*} factor is given the same relative error as calculated for the γ_D .
 67. B. Barish *et al.* (CLEO-II), *Phys. Rev.* **D51** (1995) 1014.
 68. H. Albrecht *et al.* (ARGUS), *Phys. Lett.* **B324** (1994) 249.
 69. H. Albrecht *et al.* (ARGUS), *Z. Phys.* **C57** (1993) 533.
 70. D. Buskulic *et al.* (ALEPH), Paper contributed to *this conference* and to the

EPS Conference, Brussels (1995) No.0635.

71. The DELPHI collaboration, Paper contributed to *this conference* and to the *EPS Conference, Brussels* (1995) No.0569.
72. The following results were averaged: [10%] D. Bortoletto *et al.* (CLEO-I.5) *Phys. Rev. Lett.* **63** (1989) 1667; [12%] Ref. 69 (ARGUS) (1993); [12%] Ref. 71 (DELPHI) (1995); [18%] Ref. 70 (ALEPH) (1995); [25%] Ref. 68 (ARGUS) (1994); [25%] Ref. 67 (CLEO-II) (1995). The numbers in square brackets specify weights assigned to each measurement.
73. The following results were averaged: [15%] H. Albrecht *et al.* (ARGUS), *Phys. Lett.* **B275** (1992) 195; [22%] R. Fulton *et al.* (CLEO-I.5), *Phys. Rev.* **D43** (1991) 651; [63%] Ref. 67 (CLEO-II) (1995). The numbers in square brackets specify weights assigned to each measurement.
74. M.E. Luke, *Phys. Lett.* **B252** (1990) 447.
75. S. Stone, Proceedings of the *VIII Meeting of Particles and Fields of the American Physical Society, Albuquerque* (1994) Ed. S. Seidel, World Scientific, p. 871.
76. J.E. Duboscq *et al.* (CLEO-II), Preprint CLNS 95/1372 (1995).
77. Ref. 61 and F.E. Close, A. Wambach, *Nucl. Phys.* **B412** (1994) 169, Preprint RAL-94-041 (1994).
78. The DELPHI collaboration, Paper contributed to the *XXVII Int. Conf. on High Energy Phys. Glasgow*, (1994) No.0185.
79. D. Busculic *et al.* (ALEPH), *Phys. Lett.* **B345** (1994) 103; Paper contributed to *this conference* and to the *EPS Conference, Brussels* (1995) No.0426.
80. R. Akers *et al.* (OPAL), *Z. Phys.* **C67** (1995) 57; Paper contributed to *this conference* and to the *EPS Conference, Brussels* (1995) No.0260.
81. J.P. Alexander *et al.* (CLEO-II), Paper contributed to *this conference* and to the *EPS Conference, Brussels* (1995) No.0168.
82. R. Fulton *et al.* (CLEO-I.5), *Phys. Rev. Lett.* **64** (1990) 16.
83. H. Albrecht *et al.* (ARGUS), *Phys. Lett.* **B234** (1990) 409; **B255** (1991) 297.
84. J. Bartelt *et al.* (CLEO-II), *Phys. Rev. Lett.* **71** (1993) 4111.
85. N. Isgur, D. Scora, *Phys. Rev. D* **52** (1995) 2783.
86. J.G. Körner, G.A. Schuler, *Z. Phys.* **C38** (1988) 511, erratum *Z. Phys.* **C41** (1989) 690.
87. C. Ramirez, J.F. Donoghue, G. Burdman, *Phys. Rev.* **D41** (1990) 1496.
88. R. Ammar *et al.* (CLEO-II), Paper contributed to *this conference* and to the *EPS Conference, Brussels* (1995) No.0165.
89. A. Bean *et al.* (CLEO-II), *Phys. Rev. Lett.* **70** (1993) 2681.
90. M. Wirbel, B. Stech, M. Bauere, *Z. Phys.* **C29** (1985) 637, M. Bauer, M. Wirbel, *Z. Phys.* **C42** (1989) 671.